

# Simultaneous Aerosol Mass Spectrometry and Chemical Ionisation Mass Spectrometry measurements during a biomass burning event in the UK: Insights into nitrate chemistry

5 Ernesto Reyes-Villegas<sup>1</sup>, Michael Priestley<sup>1</sup>, Yu-Chieh Ting<sup>1</sup>, Sophie Haslett<sup>1</sup>, Thomas Bannan<sup>1</sup>,  
Michael Le Breton<sup>1\*</sup>, Paul I. Williams<sup>1,2</sup>, Asan Bacak<sup>1</sup>, Michael J. Flynn<sup>1</sup>, Hugh Coe<sup>1</sup>, Carl Percival<sup>1Δ</sup>,  
James D. Allan<sup>1,2</sup>

<sup>1</sup>School of Earth, Atmospheric and Environmental Sciences, The University of Manchester, Manchester, M13 9PL, UK

<sup>2</sup>National Centre for Atmospheric Science, The University of Manchester, Manchester, M13 9PL, UK

10 \*Now at University of Gothenburg, 40530 Gothenburg, Sweden

<sup>Δ</sup>Now at Jet Propulsion Laboratory, 4800 Oak Grove Drive, Pasadena, CA 91109, USA

*Correspondence to:* Ernesto Reyes-Villegas (ernesto.reyesvillegas@manchester.ac.uk)

**Abstract.** Over the past decade, there has been an increasing interest in short-term events that negatively affect air quality such as bonfires and fireworks. High aerosol and gas concentrations generated from public bonfires/fireworks were measured in order to understand the night-time chemical processes and their atmospheric implications. Nitrogen chemistry was observed during the Bonfire Night with nitrogen containing compounds in both gas and aerosol phase and further N<sub>2</sub>O<sub>5</sub> and ClNO<sub>2</sub> concentrations, which depleted early next morning due to photolysis of NO<sub>3</sub> radicals, ceasing production. Particulate organic oxides of nitrogen (PON) concentrations of 2.8 μg.m<sup>-3</sup> were estimated using the m/z 46:30 ratios from AMS measurements, according to previously published methods. ME-2 source apportionment was performed to determine organic aerosol concentrations from different sources after modifying the fragmentation table and it was possible to identify two PON factors representing primary (pPON\_ME2) and secondary (sPON\_ME2) contributions. A slight improvement in the agreement between the source apportionment of the AMS and a collocated AE-31 Aethalometer was observed after modifying the prescribed fragmentation in the AMS organic spectrum (the fragmentation table) to determine PON sources, which resulted in an r<sup>2</sup> = 0.894 between BBOA and *b<sub>abs\_470wb</sub>* compared to an r<sup>2</sup> = 0.861 obtained without the modification. Correlations between OA sources and measurements made using Time of Flight Chemical Ionization Mass Spectrometry with an iodide adduct ion were performed in order to determine possible gas tracers to be used in future ME-2 analyses to constrain solutions. During Bonfire Night, strong correlations (r<sup>2</sup>) were observed between BBOA and methacrylic acid (0.92), acrylic acid (0.90), nitrous acid (0.86), propionic acid, (0.85) and hydrogen cyanide (0.76). A series of oxygenated species, chlorine compounds showed good correlations with sPON\_ME2 and the low volatility oxygenated organic aerosol (LVOOA) factor during Bonfire Night and an event with low pollutant concentrations. Further analysis of pPON\_ME2 and sPON\_ME2 was performed in order to determine whether these PON sources absorb light near the UV region using an Aethalometer. This hypothesis was tested by doing multilinear regressions between *b<sub>abs\_470wb</sub>* and BBOA, sPON\_ME2 and pPON\_ME2. Our results suggest that sPON\_ME2 does not absorb light at 470 nm while pPON\_ME2 and LVOOA absorb light at 470 nm. This may inform black carbon (BC) source apportionment studies from Aethalometer measurements, through investigation of the brown carbon contribution to *b<sub>abs\_470wb</sub>*.

## 1. Introduction.

Exposure to combustion aerosols has been associated with a range of negative health effects. In particular, wood smoke aerosols have been shown to present respiratory and cardiovascular health effects (Naeher et al., 2007). Bonfires and fireworks are one of the main sporadic events with high emissions of atmospheric pollutants (Vassura et al., 2014; Joshi et

40 al., 2016), even when these high emissions only last a couple of hours, high pollutant concentrations may instigate adverse effects on human health (Moreno et al., 2007; Godri et al., 2010) and severely reduce visibility (Vecchi et al., 2008). Ravindra et al. (2003) found that the short-term exposure to air pollutants increases the likelihood of acute health effects.

Due to these adverse effects, different studies have been performed to analyse air pollution during important festivities around the world, for instance New Year's Eve celebrations (Drewnick et al., 2006; Zhang et al., 2010), the Lantern Festival 45 in China (Wang et al., 2007) and Diwali festival in India (Pervez et al., 2016) as well as football matches such as during the Bundesliga in Mainz, Germany in 2012 (Faber et al., 2013). In the UK, the Bonfire Night festivity takes place on November 5<sup>th</sup> to commemorate Guy Fawkes' unsuccessful attempt to destroy the Houses of Parliament in 1605 (Ainsworth, 1850). During this celebration, bonfires usually followed by fireworks, are lit domestically and on a larger scale communally in public parks. Different studies have been carried out to assess the air pollution during Bonfire Night in the UK; for instance 50 targeting the particle size distribution (Colbeck and Chung, 1996), investigating PM<sub>10</sub> concentrations in different cities around the UK during Bonfire Night celebrations (Clark, 1997), measuring dioxins in ambient air in Oxford (Dyke et al., 1997); polycyclic aromatic hydrocarbons were measured in Lancaster, 2000 (Farrar et al., 2004) and potentially toxic elements were measured and their association to health risks was assessed in London (Hamad et al., 2015).

Receptor modelling has been widely used to determine OA sources in urban environments. However, it has been used in just 55 a small number of studies with sporadic events of high pollutant concentrations. For instance, Vecchi et al. (2008) were the first to analyse measurements taken during firework displays using positive matrix factorisation (PMF). Tian et al. (2014) did a PMF analysis of PM<sub>2.5</sub> components, identifying five different sources: Crustal dust, coal combustion, secondary particles, vehicular exhausts and fireworks. In Riccione, Italy, Vassura et al. (2014) determined that levoglucosan, OC, PAHs, Al, and Pb, emitted from bonfires during St. Joseph's Eve, can be used as markers for bonfire emissions.

60 Particulate organic oxides of nitrogen (PON), a term we use here to encompass nitro-organics and organic nitrates, have been found to absorb light near the UV region (Mohr et al., 2013) and to present potential toxicity to human health (Fernandez et al., 1992; Qingguo et al., 1995). PON also act as a NO<sub>x</sub> reservoir at night, releasing NO<sub>x</sub> concentrations when the sun rises with the possibility of increasing O<sub>3</sub> production (Perring et al., 2013; Mao et al., 2013). PON are important components of organic aerosols; for instance Day et al. (2010), in measurements taken during winter at an urban location, found that PON 65 concentrations accounted for up to 10% of organic matter. Kiendler-Scharr et al. (2016) concluded that, at a continental scale, PON represent 34% to 44% of aerosol nitrate. Organic oxides of nitrogen can be categorised, according to their origin, into two types; primary and secondary, primary organic nitrates are related to combustion sources (Zhang et al., 2016) such as fossil fuel (Day et al., 2010) and biomass burning emissions (Kitanovski et al., 2012; Mohr et al., 2013). Secondary organic oxides of nitrogen are produced in the atmosphere, for example when NO<sub>3</sub> reacts with unsaturated hydrocarbons (Ng et al., 2017). Nitrophenols are produced from reactions of phenols, both during the day reacting with OH + NO<sub>2</sub>, and at night 70 reacting with NO<sub>3</sub> + NO<sub>2</sub> (Harrison et al., 2005; Yuan et al., 2016).

The Aethalometer (Magee Scientific, USA) has been widely used to measure light absorbing carbon, proving to be a robust instrument that can operate in a variety of environments and is currently being used at many different locations around the world. The European Environment Agency, in a technical report published in 2013 (EEA, 2013), states that there are at least 75 11 European countries using Aethalometers. The UK has a black carbon (BC) network comprising 14 sites covering a wide range of monitoring sites (<https://uk-air.defra.gov.uk/networks/network-info?view=ukbsn>) and, in 2016, India started a BC network with 16 Aethalometers (LASKAR et al., 2016). Commonly, Aethalometers have been used to separate sources of light-absorbing aerosols following Sandradewi et al. (2008). The approach separates absorption from traffic, predominately resulting from BC, which absorbs light in the infrared region and from wood burning, which includes BC and absorbing 80 organic matter that also absorbs near the ultraviolet region. The Aethalometer model is based on the differences of aerosol

absorption, using the absorption Ångström exponent, at a specific wavelength of light chosen to run the model. Absorption Ångström exponent values range from 0.8-1.1 for traffic and 0.9-3.5 for wood burning (Zotter et al., 2017). It is known that Brown Carbon (BrC) is organic matter capable of absorbing light near the UV region (Bones et al., 2010; Saleh et al., 2014) and that PON is a potential contributor to BrC (Mohr et al., 2013). However, the mechanistic behaviour that links this  
85 behaviour to wood burning has not completely been resolved and there may be other sources such as secondary organic aerosols that can absorb near the UV region.

Here we present an analysis performed on data collected during Bonfire Night celebrations in Manchester, UK (29th October to 10th November 2014) using a cToF-AMS and a HR-ToF-CIMS along with other instruments to measure both aerosols and gaseous pollutants with the aim of understanding the night-time chemical processes and their atmospheric implications.  
90 Very high concentrations of pollutants occurred as a result of the meteorological conditions, which presented a good opportunity to investigate the detailed phenomenon as a case study, particularly the possibility to determine PON concentrations, their nature and interaction with Aethalometer measurements.

## 2. Methods

### 2.1 Site and instrumentation

95 Online measurements of aerosols and gases were taken from ambient air, between 29<sup>th</sup> October and 10<sup>th</sup> November 2014, at a rooftop location at the University of Manchester [53.467° N, 2.232° W], in order to quantify atmospheric pollution during Bonfire Night celebrations on and around 5<sup>th</sup> November. Figure S1 shows a map with the location of the monitoring site and nine public parks where bonfire/fireworks were displayed around greater Manchester. This is the same dataset presented by Liu et al. (2017).

100 A compact Time of Flight Aerosol Mass Spectrometer (cToF-AMS, hereafter AMS) was used to perform 5-minute measurements of organic aerosols (OA), sulfate (SO<sub>4</sub><sup>2-</sup>), nitrate (NO<sub>3</sub><sup>-</sup>), ammonium (NH<sub>4</sub><sup>+</sup>) and chloride (Cl<sup>-</sup>) (Drewnick et al., 2005). This version of AMS provides unit mass resolution mass spectra information. A High Resolution Time of Flight Chemical Ionization Mass Spectrometer (HR-ToF-CIMS, hereafter CIMS) was used to measure gas phase concentrations, using iodide as a reagent (Lee et al., 2014). The methodology to calculate gas phase concentrations from CIMS  
105 measurements are been described by Priestley et al. (In preparation). An Aethalometer, model AE31 (Magee Scientific), measured light absorption at seven wavelengths (370, 450, 571, 615, 660, 880 and 950 nm) and a Multi Angle Absorption Photometer (MAAP; Thermo Model 5012) measured BC concentrations (Petzold et al., 2002). NO<sub>x</sub>, CO, O<sub>3</sub> and meteorology data were downloaded from Whitworth observatory (<http://www.cas.manchester.ac.uk/restools/whitworth/data/>), which were measured at the same location. From 31<sup>st</sup> October  
110 to 10<sup>th</sup> November, a catalytic stripper was attached to the AMS, switching every 30 minutes between direct measurements and through the catalytic stripper. These measurements were performed as part of a different experiment (Liu et al., 2017). In the present study we used the AMS data from the direct measurements only, aerosol and gas data from other instruments were averaged to AMS sampling times.

### 2.2 Source apportionment

#### 115 2.2.1 Aethalometer model

The aerosol light absorption depends on the wavelength and may be used to apportion BC from traffic and wood burning from Aethalometer measurements as proposed by (Sandradewi et al., 2008). The absorption coefficients ( $b_{abs}$ ) are related to

the wavelengths at which the absorptions are measured ( $\lambda$ ) and Ångström absorption exponents ( $\alpha$ ) with the relationship:  $b_{abs} \propto \lambda^{\alpha}$ , thus the following equations can be solved:

$$120 \quad \frac{b_{abs\_470tr}}{b_{abs\_950tr}} = \left(\frac{470}{950}\right)^{-\alpha_{tr}} \quad (1)$$

$$\frac{b_{abs\_470wb}}{b_{abs\_950wb}} = \left(\frac{470}{950}\right)^{-\alpha_{wb}} \quad (2)$$

$$b_{abs}(470_{nm}) = b_{abs\_470tr} + b_{abs\_470wb} \quad (3)$$

$$125 \quad b_{abs}(950_{nm}) = b_{abs\_950tr} + b_{abs\_950wb} \quad (4)$$

Here, it is possible to calculate the wood burning (wb) and traffic (tr) contributions to BC at 470 and 950 nanometres (nm) as used in previous studies (Crilley et al., 2015; Harrison et al., 2012). Wavelengths 470 and 950 nm were chosen as Zotter et al. (2017) determined that using this pair of wavelength resulted in fewer residuals compared when using the pair of wavelengths 470-880, and 370-880 nm. Before the Aethalometer model was applied, the absorption coefficients ( $b_{abs}$ ) needed to be corrected following Weingartner et al. (2003) as attenuation is affected by scattering and loading variations. The following parameters were calculated: multiple scattering constant  $C = 3.16$  and filter loading factors ( $f$ ) of 1.49 and 1.28 for the wavelengths 470 and 950 nm respectively. Refer to section S3 in supplement for detailed information.

### 2.2.2 Particulate Organic Oxides of Nitrogen (PON)

135 Concentrations of PON were calculated following the method proposed by Farmer et al. (2010) and the considerations used by Kiendler-Scharr et al. (2016). This method has been previously used in studies looking at aerosols from biomass burning (Tiitta et al., 2016; Zhu et al., 2016; Florou et al., 2017). Equation 5 calculates the PON fraction ( $X_{PON}$ ), using the signals at  $m/z$  30 and  $m/z$  46 to calculate  $m/z$  ratios 46:30 from AMS measurements ( $R_{meas}$ ), from ammonium nitrate calibrations ( $R_{cal}$ ), and from organic nitrogen ( $R_{ON}$ ) to quantify PON concentrations.

$$140 \quad X_{PON} = \frac{(R_{meas} - R_{cal})(1 + R_{ON})}{(R_{ON} - R_{cal})(1 + R_{meas})} \quad (5)$$

Where ratios from ammonium nitrate calibrations  $R_{cal} = 0.5$ ;  $R_{meas} = m/z$  46:30 ratio from measurements;  $m/z$  46:30 ratio from ON  $R_{ON} = 0.1$ , Following Kostenidou et al. (2015) consideration,  $R_{ON} = 0.1$  was calculated as the minimum  $m/z$  46:30 ratio observed.  $R_{ON}$  value of 0.1 has been used in previous studies (Kiendler-Scharr et al., 2016; Tiitta et al., 2016).

$$PON = X_{PON} * NO_3^- \quad (6)$$

145 Finally, equation 6 calculates PON concentrations [ $\mu\text{g}\cdot\text{m}^{-3}$ ] where  $NO_3^-$  is the total nitrate measured by the cToF-AMS. The method proposed by Farmer et al. (2010) is based on HR-ToF-AMS measurements where  $m/z$  30 represents  $NO^+$  ion and  $m/z$  46  $NO_2^+$  ion while the cToF-AMS gives unit mass resolution mass spectra information, hence, there is the possibility to have interference of  $CH_2O^+$  ion at  $m/z$  30. However, when analysing mass spectra from previous laboratory and ambient studies using HR-ToF-AMS to investigate biomass burning emissions, we can confirm that the signal of  $CH_2O^+$  at  $m/z$  30 is low compared to signals at  $m/z$ 's 29 and 31, while in this study  $m/z$  30 is the main signal (Fig. 5.c). Hence, in this study an interference of  $CH_2O^+$  at  $m/z$  30 is unlikely and if there were any interference of  $CH_2O^+$  it would be negligible. Table S1 in supplement shows  $m/z$  30/29 and 30/31 from previous laboratory and ambient studies investigating biomass burning emissions.

Another possible interference would be the presence of mineral nitrates at  $m/z$  30 (e.g.  $\text{KNO}_3$  and  $\text{NaNO}_3$ ). However, mineral nitrate salts tend to be large particles (Allan et al., 2006;Chakraborty et al., 2016) and also have low vaporisation efficiency (Drewnick et al., 2015), which makes it unlikely to be measured by the AMS in large quantities.

### 2.2.3 Multilinear engine 2 (ME-2)

Multilinear engine 2 (Paatero, 1999) is a multivariate solver used to determine factors governing the behaviour of a two dimensional data matrix, which then can be interpreted as pollutant sources. ME-2 uses the same data model as PMF, which is also a receptor model that performs factorisation by using a weighted least squares approach (Paatero and Tapper, 1994).

In order to explore the solution space, ME-2 is capable of using information from previous studies, for example, pollutant time series or mass spectra, as inputs to the model (named target time series and target profiles respectively) to constrain the runs. These constraints are performed using the a-value approach, to determine the extent to which the output is allowed to vary. For example, by using an a-value of 0.1 to a specific source, the user is allowing the output to vary 10% from the input. For more details refer to Canonaco et al. (2013).

In this study, ME-2 and PMF were used through the source finder interface, SoFi version 4.8 (Canonaco et al., 2013) to identify OA sources using the suggestions made by Crippa et al. (2014) and the strategy proposed by Reyes-Villegas et al. (2016). ME-2 was performed using mass spectra (BBOA, HOA and COA) from two different studies as target profiles (TP) to constrain the runs; London (Young et al., 2015) and Paris (Crippa et al., 2013), Figure S5 explains the labelling used to identify the different runs.

Solutions were explored with PMF using different  $f_{\text{peak}}$  values (ranging from -1.0 to 1.0 with steps of 0.1) and ME-2 using different a-values, (nine runs with London TP and nine runs with Paris TP), looking at four, five and six-factor solutions. Section S7.1 shows the strategy used to determine the optimal solution. Factorisation struggles to separate two or more sources if they are highly correlated, for example during stagnant conditions due to low temperatures and wind speed, which was the case during Bonfire Night 2014. The pollutants were well-mixed, making it difficult to separate the sources. Hence, four tests were performed using different time sets in order to identify the best way to perform source apportionment:

- Test 1 performs factorisation on all the dataset.
- Test 2 involves factorising the event before and after Bonfire Night and using mass spectra from this analysis as TP to factorise the Bonfire Night event.
- Test 3 involves factorising the Bonfire Night event and using mass spectra from this analysis as TP as applied to the complete dataset.
- Test 4 involves factorising the event before and after Bonfire Night and using mass spectra from this analysis as TP to factorise the full dataset.

PON may exhibit covariance with other types of OA, thus their inclusion in the source apportionment analysis may improve the factorisation and highlight their co-emission with other OA types. Previous studies have quantified PON concentrations from AMS-PMF analysis to both rural and urban measurements (Sun et al., 2012;Hao et al., 2014;Xu et al., 2015;Zhang et al., 2016). In this study, an experiment was designed by modifying the fragmentation table, through the AMS analysis toolkit 1.56, in order to identify a PON source. The fragmentation table contains the different chemical species measured by the AMS, with each row representing  $m/z$  for specific species and where the user can define peaks that exist in each species' partial mass spectrum and their dependency on other peaks (Allan et al., 2004). The following steps were performed to modify the fragmentation table:

- Time series of a new ratio named  $R_{ON\_30}$  is calculated by  $R_{ON\_30} = \text{PON}/\text{mz}30$ , where PON is the time series calculated in section 2.2.2 and mz30 is the time series of the signal at  $m/z=30$  measured by the AMS.
- Using the AMS analysis toolkit; the fragmentation table is modified, in the column frag\_Organic at the  $m/z$  30, by multiplying  $R_{ON\_30} * 30$ . See figure S4 in supplement for a screenshot of the fragmentation table.
- PMF inputs are generated to be used in SoFi software.

### 3. Results

#### 3.1 Meteorology and pollutant overview

During Bonfire Night festivities on November 5<sup>th</sup>, a temperature of 4 °C and wind speed of 1.5 m.s<sup>-1</sup> were observed (Fig. 1.a), causing stagnant conditions which facilitated pollutant accumulation. Looking at the time series for the whole sampling time (Fig. 1.b), it was possible to observe four separate events with different pollutant behaviour (marked with coloured lines over the x-axis in Fig. 1), driven by different meteorological conditions: one event had high secondary concentrations (HSC, yellow line) from October 30<sup>th</sup> to November 1<sup>st</sup>, which experienced a relatively high temperature of 17-20 °C; one event of low pollutant concentrations (LC, grey line) from November 1<sup>st</sup> - 3<sup>rd</sup> was observed when continental air masses were present; Bonfire Night (bfo, blue line), with a temperature of 4 °C; and a winter-like episode (WL, purple line) from November 8<sup>th</sup> - 10<sup>th</sup>, with temperatures of 5-6 °C and high primary pollutant concentrations. Figure S3 in supplement shows back trajectories of the different events.

Aerosol concentrations during Bonfire Night were particularly high (Fig. 1.c), with the highest peak concentrations of 65.0, 19.0, 6.8, 6.0, 5.9 and 3.2  $\mu\text{g}\cdot\text{m}^{-3}$  for OA, BC, SO<sub>4</sub>, Cl, NH<sub>4</sub> and NO<sub>3</sub> respectively measured around 20:30 hrs on November 5<sup>th</sup>. It is worth noting how high these concentrations are compared to concentrations before and after Bonfire Night (Fig. 1.b) where aerosol concentrations ranged from 0.5 – 7.0  $\mu\text{g}\cdot\text{m}^{-3}$ . Measured PM<sub>1</sub> concentrations (sum of BC, organic and inorganic aerosols) of 115  $\mu\text{g}\cdot\text{m}^{-3}$  (Fig. 1.c) were observed during Bonfire Night.

Looking at the daily concentrations (Fig. 1.d), it is possible to observe PM<sub>1</sub> daily concentrations of 25  $\mu\text{g}\cdot\text{m}^{-3}$  on Bonfire Night compared to the low concentrations observed between November 1<sup>st</sup> – 2<sup>nd</sup> with concentrations ranging between 3-4  $\mu\text{g}\cdot\text{m}^{-3}$ . The impact of the emissions during Bonfire Night is present even during the next day with PM<sub>1</sub> concentrations of 14  $\mu\text{g}\cdot\text{m}^{-3}$ .

Gas phase pollutants were measured at the Whitworth observatory. Figure 2 shows high SO<sub>2</sub>, CO and NO<sub>x</sub> concentrations during Bonfire Night; these primary pollutants are well known combustion related pollutants. The high SO<sub>2</sub> concentrations during Bonfire Night are expected as solid fuels such as wood emit SO<sub>2</sub> when burned. This can also explain the SO<sub>2</sub> peak in the night of November 10<sup>th</sup> - 11<sup>th</sup> when SO<sub>2</sub> concentrations may be related to solid fuels used for domestic heating as a result of the low temperatures (6 °C). CO and NO were present at higher concentrations during Bonfire Night compared to previous days with concentrations reaching 1600 ppb (CO) 99 ppb (NO) during Bonfire Night compared to November 1<sup>st</sup> with concentrations of 230 ppb of CO and 16 ppb of NO. Some O<sub>3</sub> concentrations were measured during Bonfire Night, but given the very high NO concentrations, these are considered to be an interference with the measurement.

**3.2.1 Traffic and wood burning contributions to BC**

OA concentrations started increasing at 19:30 hrs while BC concentrations started increasing two hours earlier around 17:00 hrs (Fig. 1.c). This rise in BC concentrations may be due to bonfire emissions, although they may also be related to traffic emissions; thus the Aethalometer model was used to identify both traffic and wood burning contributions to BC.

230 Once,  $b_{abs}$  values are corrected, equations shown in section 2.2.1 are used to apply the Aethalometer model, with Ångström absorption exponents ( $\alpha$ ) of 1.0 for traffic ( $\alpha_{tr}$ ), using the wavelength 470 nm, and 2.0 for wood burning ( $\alpha_{wb}$ ) using the wavelength 950 nm, to determine traffic and wood burning contributions. Figure 3 shows the absorption coefficients for wood burning  $b_{abs\_470wb}$  (blue) and traffic  $b_{abs\_950tr}$  (red), both increasing around 17:00-18:00 hrs to values lower than 100  $Mm^{-1}$  while  $b_{abs}$ , indicating contributions from wood burning and traffic during this event. It is when the majority of bonfire events are taking place, around 20:00, when  $b_{abs\_470wb}$  shows the greatest increase, with values reaching 480  $Mm^{-1}$  compared to 150  $Mm^{-1}$  for  $b_{abs\_950tr}$ .

**3.2.2 PON identification and quantification**

Currently, there is not a direct technique to quantify on-line integrated PON concentrations. However, it is possible to estimate PON concentrations from AMS measurements using the m/z 46:30 ratios (Farmer et al., 2010) as explained in section 2.2.2. This event during Bonfire Night 2014, with high pollutant concentrations, provided the opportunity to identify the presence of PON. Inorganic nitrate from  $NH_4NO_3$  has been detected at m/z 46:30 ratios between 0.33 and 0.5 (Alfarra et al., 2006) and of 0.37 (Fry et al., 2009), although each instrument-specific ratio is determined during routine calibrations. PON has been identified with m/z 46:30 ratios of 0.07-0.10 (Hao et al., 2014) and 0.17-0.26 (Sato et al., 2010). In this study, m/z 46:30 ratios of 0.11-0.18 were observed during Bonfire Night (Fig. 4), confirming the presence of PON during this event. Figure 4 shows PON concentrations of up to 2.8  $\mu g.m^{-3}$  during Bonfire Night, which are over the detection limit of 0.1  $\mu g.m^{-3}$  reported by Bruns et al. (2010). PON concentrations are considered high compared to previous studies with concentrations between 0.03-1.2  $\mu g.m^{-3}$ , from a wide variety of sites across Europe (Kiendler-Scharr et al., 2016), while high PON concentrations of 4.2  $\mu g.m^{-3}$  were observed during a biomass burning event in Beijing, China (Zhang et al., 2016).

**3.3 OA source apportionment**

250 This event with high pollutant concentrations during Bonfire Night gave the opportunity to test ME-2 factorisation tool under these conditions and determine the best way to perform OA source apportionment on a case study event such as this. A number of different approaches to determining the optimal apportionment were tried and the one that yielded the most statistically optimal version treated as a 'best estimate', although it is acknowledged that even this may not be perfect. Indeed, it may not be possible to describe this data completely using the PMF data model. Six different tests were compared; 255 four tests before modifying the fragmentation table and two tests when modifying the fragmentation table to determine a PON source. Test2\_ON was the optimal 'best estimate' solution, a brief description is given here after being compared to the other tests (Section S7.2 in supplement). From this analysis, test2 resulted in being the best way to deconvolve OA sources, with the lowest parameters analysed: residuals, Q/Qexp values and Chi square. After modifying the fragmentation table, Test2\_ON still shows a good performance with low parameters (Fig. S6-S8). Refer to section S7 in supplementary material for detailed information about source apportionment strategy and analysis performed to determine the optimal solution. 260

Two steps were involved in Test2\_ON: in step a, PMF/ME-2 were run for the event before and after the Bonfire Night (named as not bonfire event, nbf). In Step b, mass spectra from the solution identified in step a were used as TP, to analyse the bonfire-only (bfo) event. Finally, both solutions (nbf and bfo) were merged for further analysis. Different OA sources

were identified in Test2\_ON (Fig. 5), five sources were identified during nbf event: biomass burning OA (BBOA), hydrocarbon-like OA (HOA), cooking OA (COA), secondary particulate organic oxides of nitrogen (sPON\_ME2) and low volatility OA (LVOOA). These sources are identified by characteristic peaks at their mass spectrum; BBOA, which is generated during the combustion of biomass, has a peak at  $m/z$  60, related to levoglucosan (Alfarra et al., 2007); HOA, related to traffic emissions, presents high signals at  $m/z$  55 and  $m/z$  57 typical of aliphatic hydrocarbons (Canagaratna et al., 2004); COA, emitted from food cooking activities, is similar to HOA with a higher  $m/z$  55 and lower  $m/z$  57 (Allan et al., 2010; Slowik et al., 2010; Mohr et al., 2012); LVOOA, identified as a secondary organic aerosol, has a high signal at  $m/z$  44 dominated by the  $\text{CO}_2^+$  ion (Ng et al., 2010); sPON\_ME2 has a strong signal at  $m/z$  30 and it has been identified to be secondary as it follows the same trend as LVOOA (Figure 5.a). In the case of the bfo event, six different sources were identified: BBOA, HOA, COA, LVOOA and two factors with peaks at  $m/z$ 30, which is related to PON (Sun et al., 2012). These two PON factors may have different sources; one may be secondary (sPON\_ME2) and the other primary (pPON\_ME2) which has a similar trend as BBOA (Fig. 5.b). Further details about pPON\_ME2 and sPON\_ME2 nature will be explored in section 4.2.

## 4. Discussion

### 4.1 OA source apportionment during bfo event.

It is worth noting that, while all sources have their characteristic peaks and no apparent mass spectral ‘mixing’ between sources (for example COA with a signal at  $m/z$  60), COA, HOA and LVOOA present high concentrations during Bonfire Night (Fig. 5.b). High concentrations of these sources could be expected as these (traffic and cooking activities) increase before and after the main bonfire events and the night represented a very strong inversion (which will trap all pollutants), but given the high concentrations experienced during the event and known variability for biomass burning emissions, the ‘model error’ and thus rotational freedom is likely to be substantial. The result is that these two factors could contain indeterminate contributions from minor variabilities within the biomass burning profile and therefore must be interpreted with caution.

$b_{abs\_470wb}$  has the same source as BBOA, thus the correlation between these two can be used to evaluate the effectiveness of BBOA deconvolution from OA concentrations (Frohlich et al., 2015; Visser et al., 2015),  $r^2$  values are calculated and analysed using the following considerations: Strong correlation  $r^2 \geq 0.75$ , moderate correlation  $0.5 < r^2 < 0.75$  and low correlation  $r^2 \leq 0.5$ . Here  $r^2$  values are calculated for the bfo event between  $b_{abs\_470wb}$  and the two BBOA obtained; BBOA, obtained without modifying the fragmentation table and BBOA\_2 obtained after modifying the fragmentation table to identify a PON factor. A slightly higher correlation between  $b_{abs\_470wb}$  and BBOA\_2 was observed with  $r^2 = 0.880$  compared to  $r^2 = 0.839$  for  $b_{abs\_470wb}$  and BBOA. While both have strong correlations from a quantitative point of view, qualitatively, there is an improvement in BBOA\_2. This improvement in BBOA\_2 is explained by the fact that the PON factor may be mixed with BBOA and when both sources are separated a higher correlation between BBOA\_2 and  $b_{abs\_470wb}$  is present. There is the possibility the lower  $r^2$  between  $b_{abs\_470wb}$  and BBOA is due to having two BBOA factors in test2. However, an  $r^2=0.813$  between  $b_{abs\_470wb}$  and the sum of BBOA+BBOA\_1 is still lower than 0.880.

This shows the importance of performing OA source apportionment using different approaches in order to identify the best way to deconvolve OA sources. PMF and ME-2 source apportionment tools could not completely deconvolve OA sources during the bfo event. However, due to the strong correlation between for  $b_{abs\_470wb}$  and BBOA\_2 ( $r^2 = 0.880$ ) we consider that while BBOA\_2 might not represent the total OA concentrations from the Bonfire Night event, it does represent the trend of OA emitted from the biomass burning.



## 4.2 PON Primary/secondary.

PON concentrations, obtained from the m/z ratios 46:30 (blue line in Fig. 6) have a similar trend as BBOA, both increasing at the same time, suggesting a primary origin, but after 22:00 hrs, when BBOA concentrations drop, PON concentrations remain present with a slow decrease and maintaining low concentrations when BBOA concentrations were not present anymore. This suggests the hypothesis that there might not be only one type of PON, and it could be divided into primary and secondary organic nitrate as reported in previous studies performed in western Europe (Mohr et al., 2013; Kiendler-Scharr et al., 2016).

Using this working hypothesis, primary and secondary PON concentrations were estimated using the slope between PON and BBOA, calculated from 18:00-12:00 hrs, time when the main Bonfire Night event took place (Fig. S10). PON concentrations were multiplied by this slope in order to calculate the primary PON (pPON) and secondary PON (sPON) were calculated as  $sPON = PON - pPON$ . Figure 6 shows the time series of this estimation where pPON reaches  $2.5 \mu\text{g}\cdot\text{m}^{-3}$  and sPON with concentrations of  $0.5 \mu\text{g}\cdot\text{m}^{-3}$ .

A similar behaviour with two different PON sources was observed in the source apportionment analysis performed in section 3.3, where it was possible to separate two factors with a peak at m/z 30, characteristic of PON. Figure 7 shows that around 02:00 hrs, concentrations of the pPON\_ME2 started to decrease (green line) while sPON\_ME2 concentrations (grey line) increased. This analysis shows the presence of two different types of PON; pPON\_ME2 are primarily emitted along with BBOA concentrations with the further presence of a different PON, considered to be secondary, which increase when primary pollutants start to decrease. Primary and secondary sources of PON have been previously identified from AMS-PMF analyses; Hao et al. (2014) identified PON to be secondary of nature, produced from the interaction between forest and urban emissions, while Zhang et al. (2016) determined PON to be related to primary combustion sources. In this study, it is worth noticing that the increase in sPON\_ME2 takes place around 02:00 hrs, a period when NO concentrations started decreasing and CIMS-measured  $\text{N}_2\text{O}_5$  and  $\text{ClNO}_2$  started to increase suggesting that nitrate radical chemistry was occurring (Fig. 8), which is possibly the source of the sPON, although the exact mechanism can only be speculated.

Nitrate chemistry at night is important as nitrate radicals can be the main oxidants in polluted nocturnal environments away from enhanced NO and can create reservoirs and sinks of  $\text{NO}_x$ . The main  $\text{NO}_x$  removal at night is via the uptake of dinitrogen pentoxide ( $\text{N}_2\text{O}_5$ ) into aerosols, as at night  $\text{N}_2\text{O}_5$  is formed from  $\text{NO}_3$  and  $\text{NO}_2$ . In the presence of chloride in the particle phase (e.g. in sea salt particles),  $\text{N}_2\text{O}_5$  reacts to produce nitryl chloride ( $\text{ClNO}_2$ ). In the morning, following overnight accumulation of  $\text{ClNO}_2$ , photochemical reactions take place to produce Cl and  $\text{NO}_2$ .  $\text{N}_2\text{O}_5$  and  $\text{ClNO}_2$  processing and interactions with nitrate chemistry have been previously studied in the UK (Le Breton et al., 2014a; Bannan et al., 2015). Figure 8 shows  $\text{N}_2\text{O}_5$ ,  $\text{ClNO}_2$  and  $\text{O}_3$  concentrations increasing when NO and  $\text{NO}_2$  concentrations decrease. All these processes may facilitate the sPON production at night.  $\text{N}_2\text{O}_5$  concentrations reduce quickly after the sun rises, around 08:00 hours, while  $\text{ClNO}_2$  concentrations decrease at a slower rate, with the lowest concentrations observed around 13:00 hours. Along with  $\text{NO}_3$  chemistry, it was possible to observe other nitrogen containing gases during Bonfire Night using the CIMS such as hydrogen cyanide (HCN) and Nitrous acid (HONO), which have been found to be emitted from fires (Le Breton et al., 2013; Wang et al., 2015). High HONO concentrations at night are high the next morning when HONO reacts to produce OH and NO which impacts both the OH budget and  $\text{NO}_x$  concentrations early the next morning (Lee et al., 2016).

## 4.3 OA factors and CIMS correlations

Analysing the CIMS measurements and comparing them with the OA factors, it may be possible to identify gas markers that can be used as inputs (target time series) to constrain solutions in future ME-2 analyses or as proxies when AMS data is not available. A linear regression was performed between the OA sources determined in section 3.4.1 and CIMS peaks that have

been considered positively identified (Priestley et al., in preparation), performing a coefficient of determination ( $r^2$ ) analysis for the complete dataset (ALL), and the event HSC, LC, bfo and WL. During the event HSC, none of the OA sources showed an  $r^2$  higher than 0.6. HOA did not have an  $r^2$  higher than 0.6 with any of the different events analysed. There were no specific markers identified for COA, while COA showed  $r^2$  values higher than 0.6 for bfo event, these  $r^2$ s were also observed with BBOA with even higher values. Table S4 shows the  $r^2$  values, higher or equal to 0.4, obtained in this analysis. It is worth noting that  $r^2$  values in ALL event seem to be influenced by the bfo event; this is the case for BBOA, COA and LVOOA, which show similar  $r^2$  values in both events. Thus, the analysis will be only explained for the individual events: bfo LC, and WL.

As expected, during bfo, BBOA is the OA source that shows the highest number of correlations during Bonfire Night. During the bfo episode, strong correlations ( $r^2$ ) were observed with BBOA and methacrylic acid (0.92), Acrylic acid (0.90), nitrous acid (0.86), propionic acid, (0.85) and Hydrogen cyanide (0.76), which have been previously determined as biomass burning tracers (Veres et al., 2010;Le Breton et al., 2013). Formic acid presented a strong correlation ( $r^2=0.86$ ) with BBOA during Bonfire Night; however, this value drops to 0.52 for the complete dataset, which suggests formic acid during Bonfire Night is mainly primary while formic acid concentrations measured for the whole dataset may be related to primary and secondary sources. This agrees with Le Breton et al. (2014b) who explored both primary and secondary origins of formic acid.

During the bfo event, LVOOA did not show a characteristic gas marker as all the  $r^2$  values were also observed with BBOA. This suggests two hypotheses: that the LVOOA was mixed with BBOA, in the form of humic-like material (Paglione et al., 2014), which cannot be differentiated from secondary OA in the mass spectra (Fig. 5.c); or it could also be that secondary LVOOA may actually be present at the same time as BBOA concentrations, as during high relative humidity and low temperatures, enhanced partitioning of semi-volatile material to the particle phase occurs, where subsequent oxidation and oligomerisation may occur. Moreover, due to the high aerosol concentration present during Bonfire Night, there is a greater surface available for gases to be condensed and more particulate bulk to absorb into, thus it could be speculated that there would be high secondary aerosol concentrations. However, this is deemed unlikely, as there may be little gas phase oxidation occurring in the presence of such high NO concentrations, which will remove ozone and nitrate radicals, the main source of oxidants at night.

During the bfo event, pPON\_ME2 showed strong  $r^2$  values with carbon monoxide (0.78) and hydrogen cyanide (0.77) and moderate correlations with methylformamide (0.65) and dimethylformamide (0.63), all of which are typical primary pollutants related to combustion processes [(Borduas et al., 2015) and references therein]. sPON\_ME2 showed moderate correlations with CINO<sub>2</sub> (0.52) and CINO<sub>3</sub> (0.53). Moderate  $r^2$  values were also observed during LC episode between CINO<sub>2</sub> - CINO<sub>3</sub> and LVOOA (0.67 - 0.66) and sPON (0.74 - 0.69) proving their secondary origin. Cl<sub>2</sub>, which has been previously identified to be related to both primary and secondary sources (Faxon et al., 2015), shows low correlations with pPON\_ME2 (0.44) during bfo event and sPON\_ME2 (0.55) during LC event.

#### 4.4 PON and its relationship with $b_{abs,470wb}$ and BBOA

Organic oxides of nitrogen, originating from biomass burning, have been previously found to absorb light near the UV region (Jacobson, 1999;Flowers et al., 2010;Mohr et al., 2013). However, there is still a question of whether this absorption is due to primary or secondary PON. Here, the relationship between  $b_{abs,470wb}$  and PON and BBOA will be analysed to determine if sPON absorbs at 470  $Mm^{-1}$ , which would interfere with Aethalometer measurements.

In order to quantitatively determine any contribution from PON to the Aethalometer data products, a multilinear regression (MLR) analysis was performed on the complete dataset (ALL), and the events HSC, LC, bfo and WL (Table 1). This

analysis was done in three ways: A multilinear regression (MLR1) with BBOA from organic aerosol source apportionment without modifying the FragPanel and PON from m/z 46:30 analysis; A multilinear regression (MLR2) with BBOA\_2 from organic aerosol source apportionment after modifying the FragPanel and PON from 46:30 analysis; A multilinear regression (MLR3) with with BBOA\_2 and PON sources from organic aerosol source apportionment after modifying the FragPanel. The following bilinear regression was used:

$$b_{abs\_470wb} = A + B * x_1 + C * x_2 \quad (7)$$

With  $x_1$ =BBOA and  $x_2$ =PON for MLR1;  $x_1$ =BBOA\_2 and  $x_2$ =PON for MLR2;  $x_1$ = BBOA\_2 and  $x_2$ =sPON\_ME2 for MLR3. Additionally, a trilinear regression was performed to \*HSC and \*bfo with  $x_3$ =LVOOA in \*HSC and  $x_3$ = pPON in \*bfo. A is the origin and the partial slopes B, C and D represent the contribution of  $x_1$ ,  $x_2$  and  $x_3$  to  $b_{abs\_470wb}$ , respectively.

As used in previous studies (Elser et al., 2016; Reyes-Villegas et al., 2016), multilinear regression analysis allows the relationship of one parameter between two or more variables to be determined. Here we are analysing the partial slopes and origin to determine the correlation of  $b_{abs\_470wb}$  with the other variables. Table 1 shows the MLR outputs where; A represents the background, B, C and D represent the partial slope between  $b_{abs\_470wb}$  and the respective organic aerosol. B/C represents the ratio between B and C partial slopes, with the following considerations: if  $B/C < 1$  then, there is a higher contribution of PON to  $b_{abs\_470wb}$ ; if  $B/C > 1$  then, there is a higher contribution of BBOA to  $b_{abs\_470wb}$ . Looking at the coefficient of determination of the multilinear regression ( $r^2_{MLR}$ ) for the three MLR analyses, it is possible to observe that HSC and LC events present low  $r^2_{MLR}$  values ranging from 0.064 and 0.480, while bfo and WL events have strong correlations with values between 0.760 and 0.910, which shows that is during high primary OA emissions are present when a strong correlation between  $b_{abs\_470wb}$  and BBOA and PON is observed.

These high  $r^2$  values, particularly during the bfo event which presented the highest  $r^2$  (0.910), are consistent with previous studies that found organic nitrates to absorb at short wavelengths; Mohr et al. (2013) identified correlation values of 0.65 between nitrophenols and  $b_{abs\_370wb}$ . Teich et al. (2017), in a recent study from offline filters, determined nitrated aerosol concentrations with further analysis of the light absorption of aqueous filter extracts ( $b_{abs\_370}$ ) and identified  $r^2$  values between  $b_{abs\_370}$  and nitrated aerosol concentrations of 0.67 to 0.74 depending on acidic or alkaline conditions respectively.

In MLR3, it is possible to observe that, during bfo event, the main contribution to  $b_{abs\_470wb}$  is attributed to both BBOA\_2 (16.657) and pPON\_ME2 (7.357) while babs:sPON\_ME-2 values were zero, with an optimum  $r^2$  of 0.910. This lack of correlation between babs and sPON is observed in the linear regression babs:sPON\_ME2 with an  $r^2$  of 0.188. These results show that while there is evidence of pPON\_ME2 absorbing at 470 nm, with a partial slope of 16.657, sPON\_ME2 did not show to be absorbing at 470 nm. The implication of the background not going to zero (6.093) is that there is still an unexplained contribution to the absorption at 470 nm, unrelated to sPON\_ME2.

In order to further explore the possibility of sPON\_ME-2 absorbing at 470 nm, the HSC event was analysed, where sPON\_ME2 was shown to be non-absorbing at 470 nm with a partial slope of zero. On the other hand, BBOA\_2 had a partial slope of 27.288 and bkgd a value of 2.527. This background value suggests there is another component related to  $b_{abs\_470wb}$  that is not sPON. Thus, a trilinear regression was performed to \*HSC between  $b_{abs\_470wb}$  and BBOA\_2, sPON and LVOOA. Here, the background value drops to 1.649, sPON partial slope is zero and LVOOA presents a partial slope of 1.138. These results confirm that sPON do not absorb light at 470 nm while LVOOA, or at least part of the components of LVOOA, do absorb at 470 nm during the HSC event and pPON\_ME2 during the bfo event.

These results agree with previous studies that found biomass burning OA to contain important concentrations of light absorbing brown carbon (BrC) and that certain types of SOA are effective absorbers near UV light (Bones et al., 2010; Saleh

et al., 2014; Washenfelder et al., 2015). The fact that pPON\_ME2 and LVOOA were shown to be absorbing light at a short wavelength (470 nm) will have a direct impact on Aethalometer model studies; while pPON\_ME2 could be considered a component of the wood burning aerosol apportioned using the Aethalometer; it may be that there is an interference from other forms of BrC in SOA. However, this work would suggest that sPON specifically does not contribute to the latter, so a different component of LV-OOA would have to be responsible. As well as this Aethalometer interpretation, it is also worth mentioning that these findings may have implications for studies on the radiative properties of the atmosphere, as BrC is also thought to affect climate (Jacobson, 2014).

## 5. Conclusions

In order to better understand the aerosol chemical composition and variation in source contribution during periods of nocturnal pollution, online measurements of gases and aerosols were made in ambient air between 29<sup>th</sup> October and 10<sup>th</sup> November 2014, at the University of Manchester with detailed analysis of the special high pollutant concentrations during Bonfire Night celebrations on 5<sup>th</sup> November. High aerosol concentrations were observed during the Bonfire Night event with 115  $\mu\text{g}\cdot\text{m}^{-3}$  of PM<sub>1</sub>. Important nitrogen chemistry was present with high HCN, HCNO and HONO concentrations primarily emitted with the further presence of N<sub>2</sub>O<sub>5</sub> and ClNO<sub>2</sub> concentrations from nocturnal nitrate chemistry taking place after NO<sub>x</sub> concentrations decreased.

Organic aerosol source apportionment was performed using the ME-2 factorisation tool. The particular high pollutant concentrations together with the complex mix of emissions did not allow the running of ME-2 for the complete dataset, thus the dataset was divided into different events. The best way to perform source apportionment was found to be to, (a) analyse the event before and after Bonfire Night using BBOA, HOA and COA from a previous study in Paris as TP, and (b) conduct a further ME-2 analysis of the Bonfire Night event using BBOA, HOA and COA mass spectra from (a) as TP. Moreover, a slight improvement on the source apportionment was observed after modifying the fragPanel in order to identify PON sources, increasing the  $r^2$  value from linear regressions between  $b_{abs\_470wb}$  (absorption coefficient of wood burning at 470 nm) and BBOA from 0.839 to 0.880. PMF and ME-2 source apportionment tools could not completely deconvolve OA sources during the bfo event as LV-OOA, COA and HOA may be mixed with BBOA concentrations. However, due to the strong correlation between  $b_{abs\_470wb}$  and BBOA ( $r^2 = 0.880$ ) we consider that while BBOA might not represent the total OA concentrations from the Bonfire Night event, it does represent the trend of OA emitted from the biomass burning.

The combination of CIMS measurements and OA sources determined from AMS measurements provided important information about gas tracers to be used as inputs (target time series) to improve future ME-2 analyses, particularly gases correlating with BBOA, LVOOA and sPON. However, the use of these species as target time series should be used with care as their time variation is greatly affected by meteorological conditions.

The presence of two classes of PON, secondary (sPON\_ME2) and primary (pPON\_ME2), was identified both from looking at the BBOA:PON relationship and from the ME-2 analysis after modifying the FragPanel. It is clear that, during Bonfire Night, pPON\_ME2 concentrations increased when BBOA concentrations are present and sPON\_ME2 concentrations started evolving when the primary concentrations decreased.

It was determined that pPON\_ME2 absorbed light at a wavelength of 470 nm during Bonfire Night, where the multilinear regression performed between  $b_{abs\_470wb}$ , BBOA and pPON\_ME2 showed a strong  $r^2$  of 0.910, while sPON\_ME2 did not contribute to light absorption at 470nm. During the HSC episode, LVOOA showed a partial slope of 1.138 in the multilinear regression and an  $r^2$  from linear regression with  $b_{abs\_470wb}$  of 0.225, implying secondary LVOOA (associated with SOA) may be absorbing at 470 nm and sPON\_ME2 was not absorbing at this wavelength. These results will help us to understand the

460 mechanistic contributions to UV absorption in the Aethalometer and will have direct implications for source apportionment studies, which may need to be corrected for secondary organic aerosol interferences near the UV region.

## 6. Data availability

Processed data is available through the archive at the British Atmospheric Data Centre (<http://badc.nerc.ac.uk/browse/badc>), with search term 'COMPART'. Raw data is archived at the University of Manchester and is available on request.

465 **Author contributions.** Ernesto Reyes-Villegas, Michael Flynn, Hugh Coe, Carl Percival, James Allan designed the project; Ernesto Reyes-Villegas, Yu-Chieh Ting, Sophie Haslett, Thomas Bannan, Michael Le breton, Paul Williams, Asan Bacak, operated, calibrated and performed QA of instrument measurements; Ernesto Reyes-Villegas and Michael Priestley performed the data analysis; Ernesto Reyes-Villegas, Hugh Coe and James Allan wrote the paper.

470 **Acknowledgements.** This work was supported through the UK Natural Environment Research Council (NERC) through the Com-Part (grant ref: NE/K014838/1). Ernesto Reyes-Villegas is supported by a studentship by the National Council of Science and Technology-Mexico (CONACYT) under registry number 217687.

## References

- Ainsworth, W. H.: Guy fawkes; or, the gunpowder treason, Nottingham Society, 1850.
- 475 Alfarra, M. R., Paulsen, D., Gysel, M., Garforth, A. A., Dommen, J., Prévôt, A. S. H., Worsnop, D. R., Baltensperger, U., and Coe, H.: A mass spectrometric study of secondary organic aerosols formed from the photooxidation of anthropogenic and biogenic precursors in a reaction chamber, *Atmos Chem Phys*, 6, 5279-5293, 2006.
- 480 Alfarra, M. R., Prevot, A. S. H., Szidat, S., Sandradewi, J., Weimer, S., Lanz, V. A., Schreiber, D., Mohr, M., and Baltensperger, U.: Identification of the mass spectral signature of organic aerosols from wood burning emissions, *Environmental Science & Technology*, 41, 5770-5777, Doi 10.1021/Es062289b, 2007.
- Allan, J. D., Delia, A. E., Coe, H., Bower, K. N., Alfarra, M. R., Jimenez, J. L., Middlebrook, A. M., Drewnick, F., Onasch, T. B., Canagaratna, M. R., Jayne, J. T., and Worsnop, D. R.: A generalised method for the extraction of chemically resolved mass spectra from aerodyne aerosol mass spectrometer data, *J Aerosol Sci*, 35, 909-922, DOI 10.1016/j.jaerosci.2004.02.007, 2004.
- 485 Allan, J. D., Alfarra, M. R., Bower, K. N., Coe, H., Jayne, J. T., Worsnop, D. R., Aalto, P. P., Kulmala, M., Hyötyläinen, T., Cavalli, F., and Laaksonen, A.: Size and composition measurements of background aerosol and new particle growth in a finnish forest during quest 2 using an aerodyne aerosol mass spectrometer, *Atmos. Chem. Phys.*, 6, 315-327, 10.5194/acp-6-315-2006, 2006.
- 490 Allan, J. D., Williams, P. I., Morgan, W. T., Martin, C. L., Flynn, M. J., Lee, J., Nemitz, E., Phillips, G. J., Gallagher, M. W., and Coe, H.: Contributions from transport, solid fuel burning and cooking to primary organic aerosols in two uk cities, *Atmos Chem Phys*, 10, 647-668, 2010.
- Bannan, T. J., Booth, A. M., Bacak, A., Muller, J. B. A., Leather, K. E., Le Breton, M., Jones, B., Young, D., Coe, H., Allan, J., Visser, S., Slowik, J. G., Furger, M., Prevot, A. S. H., Lee, J., Dunmore, R. E., Hopkins, J. R., Hamilton, J. F., Lewis, A. C., Whalley, L. K., Sharp, T., Stone, D., Heard, D. E., Fleming, Z. L., Leigh, R., Shallcross, D. E., and Percival, C. J.: The first uk measurements of nitril chloride using a chemical ionization mass spectrometer in central london in the summer of 2012, and an investigation of the role of cl atom oxidation, *J Geophys Res-Atmos*, 120, 5638-5657, 10.1002/2014JD022629, 2015.
- 495 Bones, D. L., Henricksen, D. K., Mang, S. A., Gonsior, M., Bateman, A. P., Nguyen, T. B., Cooper, W. J., and Nizkorodov, S. A.: Appearance of strong absorbers and fluorophores in limonene-o3 secondary organic aerosol due to nh4+-mediated chemical aging over long time scales, *Journal of Geophysical Research: Atmospheres*, 115, n/a-n/a, 10.1029/2009jd012864, 2010.
- 500 Borduas, N., da Silva, G., Murphy, J. G., and Abbatt, J. P. D.: Experimental and theoretical understanding of the gas phase oxidation of atmospheric amides with oh radicals: Kinetics, products, and mechanisms, *The Journal of Physical Chemistry A*, 119, 4298-4308, 10.1021/jp503759f, 2015.

- 505 Bruns, E. A., Perraud, V., Zelenyuk, A., Ezell, M. J., Johnson, S. N., Yu, Y., Imre, D., Finlayson-Pitts, B. J., and Alexander, M. L.: Comparison of ftir and particle mass spectrometry for the measurement of particulate organic nitrates, *Environmental Science & Technology*, 44, 1056-1061, [10.1021/es9029864](https://doi.org/10.1021/es9029864), 2010.
- Canagaratna, M. R., Jayne, J. T., Ghertner, D. A., Herndon, S., Shi, Q., Jimenez, J. L., Silva, P. J., Williams, P., Lanni, T., Drewnick, F., Demerjian, K. L., Kolb, C. E., and Worsnop, D. R.: Chase studies of particulate emissions from in-use new york city vehicles, *Aerosol Science and Technology*, 38, 555-573, [10.1080/02786820490465504](https://doi.org/10.1080/02786820490465504), 2004.
- 510 Canonaco, F., Crippa, M., Slowik, J. G., Baltensperger, U., and Prevot, A. S. H.: Sofi, an igor-based interface for the efficient use of the generalized multilinear engine (me-2) for the source apportionment: Me-2 application to aerosol mass spectrometer data, *Atmos Meas Tech*, 6, 3649-3661, DOI 10.5194/amt-6-3649-2013, 2013.
- Chakraborty, A., Gupta, T., and Tripathi, S. N.: Chemical composition and characteristics of ambient aerosols and rainwater residues during indian summer monsoon: Insight from aerosol mass spectrometry, *Atmos Environ*, 136, 144-155, [10.1016/j.atmosenv.2016.04.024](https://doi.org/10.1016/j.atmosenv.2016.04.024), 2016.
- 515 Clark, H.: New directions. Light blue touch paper and retire, *Atmos Environ*, 31, 2893-2894, [10.1016/s1352-2310\(97\)88278-7](https://doi.org/10.1016/s1352-2310(97)88278-7), 1997.
- Colbeck, I., and Chung, M.-C.: Ambient aerosol concentrations at a site in se england during bonfire night 1995, *J Aerosol Sci*, 27, Supplement 1, S449-S450, [http://dx.doi.org/10.1016/0021-8502\(96\)00297-2](http://dx.doi.org/10.1016/0021-8502(96)00297-2), 1996.
- 520 Crilley, L. R., Bloss, W. J., Yin, J., Beddows, D. C. S., Harrison, R. M., Allan, J. D., Young, D. E., Flynn, M., Williams, P., Zotter, P., Prevot, A. S. H., Heal, M. R., Barlow, J. F., Halios, C. H., Lee, J. D., Szidat, S., and Mohr, C.: Sources and contributions of wood smoke during winter in london: Assessing local and regional influences, *Atmos. Chem. Phys.*, 15, 3149-3171, [10.5194/acp-15-3149-2015](https://doi.org/10.5194/acp-15-3149-2015), 2015.
- 525 Crippa, M., DeCarlo, P. F., Slowik, J. G., Mohr, C., Heringa, M. F., Chirico, R., Poulain, L., Freutel, F., Sciare, J., Cozic, J., Di Marco, C. F., Elsasser, M., Nicolas, J. B., Marchand, N., Abidi, E., Wiedensohler, A., Drewnick, F., Schneider, J., Borrmann, S., Nemitz, E., Zimmermann, R., Jaffrezo, J. L., Prevot, A. S. H., and Baltensperger, U.: Wintertime aerosol chemical composition and source apportionment of the organic fraction in the metropolitan area of paris, *Atmos Chem Phys*, 13, 961-981, DOI 10.5194/acp-13-961-2013, 2013.
- 530 Crippa, M., Canonaco, F., Lanz, V. A., Aijala, M., Allan, J. D., Carbone, S., Capes, G., Ceburnis, D., Dall'Osto, M., Day, D. A., DeCarlo, P. F., Ehn, M., Eriksson, A., Freney, E., Ruiz, L. H., Hillamo, R., Jimenez, J. L., Junninen, H., Kiendler-Scharr, A., Kortelainen, A. M., Kulmala, M., Laaksonen, A., Mensah, A., Mohr, C., Nemitz, E., O'Dowd, C., Ovadnevaite, J., Pandis, S. N., Petaja, T., Poulain, L., Saarikoski, S., Sellegri, K., Swietlicki, E., Tiitta, P., Worsnop, D. R., Baltensperger, U., and Prevot, A. S. H.: Organic aerosol components derived from 25 ams data sets across europe using a consistent me-2 based source apportionment approach, *Atmos Chem Phys*, 14, 6159-6176, DOI 10.5194/acp-14-6159-2014, 2014.
- 535 Day, D. A., Liu, S., Russell, L. M., and Ziemann, P. J.: Organonitrate group concentrations in submicron particles with high nitrate and organic fractions in coastal southern california, *Atmos Environ*, 44, 1970-1979, <http://dx.doi.org/10.1016/j.atmosenv.2010.02.045>, 2010.
- 540 Drewnick, F., Hings, S. S., DeCarlo, P., Jayne, J. T., Gonin, M., Fuhrer, K., Weimer, S., Jimenez, J. L., Demerjian, K. L., Borrmann, S., and Worsnop, D. R.: A new time-of-flight aerosol mass spectrometer (tof-ams) - instrument description and first field deployment, *Aerosol Science and Technology*, 39, 637-658, Doi 10.1080/02786820500182040, 2005.
- Drewnick, F., Hings, S. S., Curtius, J., Eerdekens, G., and Williams, J.: Measurement of fine particulate and gas-phase species during the new year's fireworks 2005 in mainz, germany, *Atmos Environ*, 40, 4316-4327, <http://dx.doi.org/10.1016/j.atmosenv.2006.03.040>, 2006.
- 545 Drewnick, F., Diesch, J. M., Faber, P., and Borrmann, S.: Aerosol mass spectrometry: Particle-vaporizer interactions and their consequences for the measurements, *Atmos. Meas. Tech.*, 8, 3811-3830, [10.5194/amt-8-3811-2015](https://doi.org/10.5194/amt-8-3811-2015), 2015.
- 550 Dyke, P., Coleman, P., and James, R.: Dioxins in ambient air, bonfire night 1994, *Chemosphere*, 34, 1191-1201, [http://dx.doi.org/10.1016/S0045-6535\(97\)00418-9](http://dx.doi.org/10.1016/S0045-6535(97)00418-9), 1997.
- EEA: Status of black carbon monitoring in ambient air in europe, 48, 2013.
- Elser, M., Huang, R. J., Wolf, R., Slowik, J. G., Wang, Q., Canonaco, F., Li, G., Bozzetti, C., Daellenbach, K. R., Huang, Y., Zhang, R., Li, Z., Cao, J., Baltensperger, U., El-Haddad, I., and André, P.: New insights into pm2.5 chemical composition and sources in two major cities in china during extreme haze events using aerosol mass spectrometry, *Atmos Chem Phys*, 16, 3207-3225, [10.5194/acp-16-3207-2016](https://doi.org/10.5194/acp-16-3207-2016), 2016.
- 555 Faber, P., Drewnick, F., Veres, P. R., Williams, J., and Borrmann, S.: Anthropogenic sources of aerosol particles in a football stadium: Real-time characterization of emissions from cigarette smoking, cooking, hand flares, and

560 color smoke bombs by high-resolution aerosol mass spectrometry, *Atmos Environ*, 77, 1043-1051, DOI 10.1016/j.atmosenv.2013.05.072, 2013.

Farmer, D. K., Matsunaga, A., Docherty, K. S., Surratt, J. D., Seinfeld, J. H., Ziemann, P. J., and Jimenez, J. L.: Response of an aerosol mass spectrometer to organonitrates and organosulfates and implications for atmospheric chemistry, *Proceedings of the National Academy of Sciences of the United States of America*, 107, 6670-6675, 10.1073/pnas.0912340107, 2010.

565 Farrar, N. J., Smith, K. E. C., Lee, R. G. M., Thomas, G. O., Sweetman, A. J., and Jones, K. C.: Atmospheric emissions of polybrominated diphenyl ethers and other persistent organic pollutants during a major anthropogenic combustion event, *Environmental Science & Technology*, 38, 1681-1685, 10.1021/es035127d, 2004.

Faxon, C., Bean, J., and Ruiz, L.: Inland concentrations of  $\text{Cl}_2$  and  $\text{ClNO}_2$  in southeast Texas suggest chlorine chemistry significantly contributes to atmospheric reactivity, *Atmosphere*, 6, 1487, 2015.

570 Fernandez, P., Grifoll, M., Solanas, A. M., Bayona, J. M., and Albaiges, J.: Bioassay-directed chemical analysis of genotoxic components in coastal sediments, *Environmental Science & Technology*, 26, 817-829, 10.1021/es00028a024, 1992.

Florou, K., Papanastasiou, D. K., Pikridas, M., Kaltsonoudis, C., Louvaris, E., Gkatzelis, G. I., Patoulias, D., Mihalopoulos, N., and Pandis, S. N.: The contribution of wood burning and other pollution sources to wintertime organic aerosol levels in two Greek cities, *Atmos. Chem. Phys.*, 17, 3145-3163, 10.5194/acp-17-3145-2017, 2017.

575 Flowers, B. A., Dubey, M. K., Mazzoleni, C., Stone, E. A., Schauer, J. J., Kim, S. W., and Yoon, S. C.: Optical-chemical-microphysical relationships and closure studies for mixed carbonaceous aerosols observed at Jeju island; 3-laser photoacoustic spectrometer, particle sizing, and filter analysis, *Atmos. Chem. Phys.*, 10, 10387-10398, 10.5194/acp-10-10387-2010, 2010.

580 Frohlich, R., Crenn, V., Setyan, A., Belis, C. A., Canonaco, F., Favez, O., Riffault, V., Slowik, J. G., Aas, W., Aijala, M., Alastuey, A., Artinano, B., Bonnaire, N., Bozzetti, C., Bressi, M., Carbone, C., Coz, E., Croteau, P. L., Cubison, M. J., Esser-Gietl, J. K., Green, D. C., Gros, V., Heikkinen, L., Herrmann, H., Jayne, J. T., Lunder, C. R., Minguillon, M. C., Mocnik, G., O'Dowd, C. D., Ovadnevaite, J., Petralia, E., Poulain, L., Priestman, M., Ripoll, A., Sarda-Estève, R., Wiedensohler, A., Baltensperger, U., Sciare, J., and Prevot, A. S. H.: Actris acsm intercomparison - part 2: Intercomparison of  $\text{me-2}$  organic source apportionment results from 15 individual, co-located aerosol mass spectrometers, *Atmos Meas Tech*, 8, 2555-2576, 10.5194/amt-8-2555-2015, 2015.

585 Fry, J. L., Kiendler-Scharr, A., Rollins, A. W., Wooldridge, P. J., Brown, S. S., Fuchs, H., Dubé, W., Mensah, A., dal Maso, M., Tillmann, R., Dorn, H. P., Brauers, T., and Cohen, R. C.: Organic nitrate and secondary organic aerosol yield from  $\text{NO}_3$  oxidation of  $\beta$ -pinene evaluated using a gas-phase kinetics/aerosol partitioning model, *Atmos. Chem. Phys.*, 9, 1431-1449, 10.5194/acp-9-1431-2009, 2009.

590 Godri, K. J., Green, D. C., Fuller, G. W., Dall'Osto, M., Beddows, D. C., Kelly, F. J., Harrison, R. M., and Mudway, I. S.: Particulate oxidative burden associated with firework activity, *Environmental Science & Technology*, 44, 8295-8301, 10.1021/es1016284, 2010.

595 Hamad, S., Green, D., and Heo, J.: Evaluation of health risk associated with fireworks activity at central London, *Air Quality, Atmosphere & Health*, 1-7, 10.1007/s11869-015-0384-x, 2015.

Hao, L. Q., Kortelainen, A., Romakkaniemi, S., Portin, H., Jaatinen, A., Leskinen, A., Komppula, M., Miettinen, P., Sueper, D., Pajunoja, A., Smith, J. N., Lehtinen, K. E. J., Worsnop, D. R., Laaksonen, A., and Virtanen, A.: Atmospheric submicron aerosol composition and particulate organic nitrate formation in a boreal forestland-urban mixed region, *Atmos Chem Phys*, 14, 13483-13495, 10.5194/acp-14-13483-2014, 2014.

600 Harrison, M. A. J., Barra, S., Borghesi, D., Vione, D., Arsene, C., and Iulian Olariu, R.: Nitrated phenols in the atmosphere: A review, *Atmos Environ*, 39, 231-248, <http://dx.doi.org/10.1016/j.atmosenv.2004.09.044>, 2005.

605 Harrison, R. M., Beddows, D. C. S., Hu, L., and Yin, J.: Comparison of methods for evaluation of wood smoke and estimation of UK ambient concentrations, *Atmos Chem Phys*, 12, 8271-8283, DOI 10.5194/acp-12-8271-2012, 2012.

Jacobson, M. Z.: Isolating nitrated and aromatic aerosols and nitrated aromatic gases as sources of ultraviolet light absorption, *J Geophys Res-Atmos*, 104, 3527-3542, DOI 10.1029/1998jd100054, 1999.

610 Jacobson, M. Z.: Effects of biomass burning on climate, accounting for heat and moisture fluxes, black and brown carbon, and cloud absorption effects, *Journal of Geophysical Research: Atmospheres*, 119, 8980-9002, 10.1002/2014jd021861, 2014.

- Joshi, M., Khan, A., Anand, S., and Sapra, B. K.: Size evolution of ultrafine particles: Differential signatures of normal and episodic events, *Environmental Pollution*, 208, Part B, 354-360, <http://dx.doi.org/10.1016/j.envpol.2015.10.001>, 2016.
- 615 Kiendler-Scharr, A., Mensah, A. A., Friese, E., Topping, D., Nemitz, E., Prevot, A. S. H., Äijälä, M., Allan, J., Canonaco, F., Canagaratna, M., Carbone, S., Crippa, M., Dall'Osto, M., Day, D. A., De Carlo, P., Di Marco, C. F., Elbern, H., Eriksson, A., Freney, E., Hao, L., Herrmann, H., Hildebrandt, L., Hillamo, R., Jimenez, J. L., Laaksonen, A., McFiggans, G., Mohr, C., O'Dowd, C., Otjes, R., Ovadnevaite, J., Pandis, S. N., Poulain, L., Schlag, P., Sellegri, K., Swietlicki, E., Tiitta, P., Vermeulen, A., Wahner, A., Worsnop, D., and Wu, H. C.: Ubiquity of organic nitrates from nighttime chemistry in the European submicron aerosol, *Geophys Res Lett*, 43, 7735-7744, 10.1002/2016gl069239, 2016.
- 620 Kitanovski, Z., Grgic, I., Vermeylen, R., Claeys, M., and Maenhaut, W.: Liquid chromatography tandem mass spectrometry method for characterization of monoaromatic nitro-compounds in atmospheric particulate matter, *J Chromatogr A*, 1268, 35-43, 10.1016/j.chroma.2012.10.021, 2012.
- 625 Kostenidou, E., Florou, K., Kaltsonoudis, C., Tsiflikiotou, M., Vratolis, S., Eleftheriadis, K., and Pandis, S. N.: Sources and chemical characterization of organic aerosol during the summer in the eastern Mediterranean, *Atmos. Chem. Phys.*, 15, 11355-11371, 10.5194/acp-15-11355-2015, 2015.
- LASKAR, S. I., JASWAL, K., BHATNAGAR, M. K., and RATHORE, L. S.: India meteorological department, India, 1021-1037, 2016.
- 630 Le Breton, M., Bacak, A., Muller, J. B. A., O'Shea, S. J., Xiao, P., Ashfold, M. N. R., Cooke, M. C., Batt, R., Shallcross, D. E., Oram, D. E., Forster, G., Bauguitte, S. J. B., Palmer, P. I., Parrington, M., Lewis, A. C., Lee, J. D., and Percival, C. J.: Airborne hydrogen cyanide measurements using a chemical ionisation mass spectrometer for the plume identification of biomass burning forest fires, *Atmos. Chem. Phys.*, 13, 9217-9232, 10.5194/acp-13-9217-2013, 2013.
- 635 Le Breton, M., Bacak, A., Muller, J. B. A., Bannan, T. J., Kennedy, O., Ouyang, B., Xiao, P., Bauguitte, S. J. B., Shallcross, D. E., Jones, R. L., Daniels, M. J. S., Ball, S. M., and Percival, C. J.: The first airborne comparison of  $\text{NO}_2$  measurements over the UK using a CIMS and BBCEAS during the RONOCO campaign, *Anal Methods-Uk*, 6, 9731-9743, 10.1039/c4ay02273d, 2014a.
- 640 Le Breton, M., Bacak, A., Muller, J. B. A., Xiao, P., Shallcross, B. M. A., Batt, R., Cooke, M. C., Shallcross, D. E., Bauguitte, S. J. B., and Percival, C. J.: Simultaneous airborne nitric acid and formic acid measurements using a chemical ionization mass spectrometer around the UK: Analysis of primary and secondary production pathways, *Atmos Environ*, 83, 166-175, <http://dx.doi.org/10.1016/j.atmosenv.2013.10.008>, 2014b.
- Lee, B. H., Lopez-Hilfiker, F. D., Mohr, C., Kurtén, T., Worsnop, D. R., and Thornton, J. A.: An iodide-adduct high-resolution time-of-flight chemical-ionization mass spectrometer: Application to atmospheric inorganic and organic compounds, *Environmental Science & Technology*, 48, 6309-6317, 10.1021/es500362a, 2014.
- 645 Lee, J. D., Whalley, L. K., Heard, D. E., Stone, D., Dunmore, R. E., Hamilton, J. F., Young, D. E., Allan, J. D., Laufs, S., and Kleffmann, J.: Detailed budget analysis of  $\text{HO}_2$  in central London reveals a missing daytime source, *Atmos. Chem. Phys.*, 16, 2747-2764, 10.5194/acp-16-2747-2016, 2016.
- 650 Liu, D., Whitehead, J., Alfarra, M. R., Reyes-Villegas, E., Spracklen, D. V., Reddington, C. L., Kong, S., Williams, P. I., Ting, Y.-C., Haslett, S., Taylor, J. W., Flynn, M. J., Morgan, W. T., McFiggans, G., Coe, H., and Allan, J. D.: Black-carbon absorption enhancement in the atmosphere determined by particle mixing state, *Nature Geosci*, 10, 184-188, 10.1038/ngeo2901, 2017.
- Mao, J., Paulot, F., Jacob, D. J., Cohen, R. C., Crouse, J. D., Wennberg, P. O., Keller, C. A., Hudman, R. C., Barkley, M. P., and Horowitz, L. W.: Ozone and organic nitrates over the eastern United States: Sensitivity to isoprene chemistry, *Journal of Geophysical Research Atmospheres*, 118, 11256-11268, 10.1002/jgrd.50817, 2013.
- 655 Mohr, C., DeCarlo, P. F., Heringa, M. F., Chirico, R., Slowik, J. G., Richter, R., Reche, C., Alastuey, A., Querol, X., Seco, R., Penuelas, J., Jimenez, J. L., Crippa, M., Zimmermann, R., Baltensperger, U., and Prevot, A. S. H.: Identification and quantification of organic aerosol from cooking and other sources in Barcelona using aerosol mass spectrometer data, *Atmos Chem Phys*, 12, 1649-1665, DOI 10.5194/acp-12-1649-2012, 2012.
- 660 Mohr, C., Lopez-Hilfiker, F. D., Zotter, P., Prevot, A. S. H., Xu, L., Ng, N. L., Herndon, S. C., Williams, L. R., Franklin, J. P., Zahniser, M. S., Worsnop, D. R., Knighton, W. B., Aiken, A. C., Gorkowski, K. J., Dubey, M. K., Allan, J. D., and Thornton, J. A.: Contribution of nitrated phenols to wood burning brown carbon light absorption in detling, United Kingdom during winter time, *Environmental Science & Technology*, 47, 6316-6324, DOI 10.1021/Es400683v, 2013.
- 665



Moreno, T., Querol, X., Alastuey, A., Cruz Minguillón, M., Pey, J., Rodriguez, S., Vicente Miró, J., Felis, C., and Gibbons, W.: Recreational atmospheric pollution episodes: Inhalable metalliferous particles from firework displays, *Atmos Environ*, 41, 913-922, <http://dx.doi.org/10.1016/j.atmosenv.2006.09.019>, 2007.

670 Naehler, L. P., Brauer, M., Lipsett, M., Zelikoff, J. T., Simpson, C. D., Koenig, J. Q., and Smith, K. R.: Woodsmoke health effects: A review, *Inhalation Toxicology*, 19, 67-106, 10.1080/08958370600985875, 2007.

Ng, N. L., Canagaratna, M. R., Zhang, Q., Jimenez, J. L., Tian, J., Ulbrich, I. M., Kroll, J. H., Docherty, K. S., Chhabra, P. S., Bahreini, R., Murphy, S. M., Seinfeld, J. H., Hildebrandt, L., Donahue, N. M., DeCarlo, P. F., Lanz, V. A., Prevot, A. S. H., Dinar, E., Rudich, Y., and Worsnop, D. R.: Organic aerosol components observed in northern hemispheric datasets from aerosol mass spectrometry, *Atmos Chem Phys*, 10, 4625-4641, DOI 10.5194/acp-10-4625-2010, 2010.

675 Ng, N. L., Brown, S. S., Archibald, A. T., Atlas, E., Cohen, R. C., Crowley, J. N., Day, D. A., Donahue, N. M., Fry, J. L., Fuchs, H., Griffin, R. J., Guzman, M. I., Herrmann, H., Hodzic, A., Iinuma, Y., Kiendler-Scharr, A., Lee, B. H., Luecken, D. J., Mao, J., McLaren, R., Mutzel, A., Osthoff, H. D., Ouyang, B., Picquet-Varrault, B., Platt, U., Pye, H. O. T., Rudich, Y., Schwantes, R. H., Shiraiwa, M., Stutz, J., Thornton, J. A., Tilgner, A., Williams, B. J., and Zaveri, R. A.: Nitrate radicals and biogenic volatile organic compounds: Oxidation, mechanisms, and organic aerosol, *Atmos Chem Phys*, 17, 2103-2162, 10.5194/acp-17-2103-2017, 2017.

680 Paatero, P., and Tapper, U.: Positive matrix factorization: A non-negative factor model with optimal utilization of error estimates of data values, *Environmetrics*, 5, 111-126, 1994.

Paatero, P.: The multilinear engine: A table-driven, least squares program for solving multilinear problems, including the n-way parallel factor analysis model, *J Comput Graph Stat*, 8, 854-888, 10.2307/1390831, 1999.

685 Paglione, M., Kiendler-Scharr, A., Mensah, A. A., Finessi, E., Giulianelli, L., Sandrini, S., Facchini, M. C., Fuzzi, S., Schlag, P., Piazzalunga, A., Tagliavini, E., Henzing, J. S., and Decesari, S.: Identification of humic-like substances (hulis) in oxygenated organic aerosols using nmr and ams factor analyses and liquid chromatographic techniques, *Atmos Chem Phys*, 14, 25-45, DOI 10.5194/acp-14-25-2014, 2014.

690 Perring, A. E., Pusede, S. E., and Cohen, R. C.: An observational perspective on the atmospheric impacts of alkyl and multifunctional nitrates on ozone and secondary organic aerosol, *Chemical Reviews*, 113, 5848-5870, 10.1021/cr300520x, 2013.

Pervez, S., Chakrabarty, R. K., Dewangan, S., Watson, J. G., Chow, J. C., and Matawle, J. L.: Chemical speciation of aerosols and air quality degradation during the festival of lights (diwali), *Atmospheric Pollution Research*, 7, 92-99, 10.1016/j.apr.2015.09.002, 2016.

695 Petzold, A., Kramer, H., and Schonlinner, M.: Continuous measurement of atmospheric black carbon using a multi-angle absorption photometer, *Environ Sci Pollut R*, 78-82, 2002.

Priestley, M., Le Breton, M., Bannan, T. J., Leather, K. E., Bacak, A., Allan, J. D., Brazier, T., Reyes-Villegas, E., Shallcross, B. M. A., Khan, M. A., De Vocht, F., D.E., S., Coe, H., and Percival, C. J.: Manchester, uk bonfire night 2014: Air quality and emission ratios during an anthropogenic biomass burning event using a time of flight chemical ionisation mass spectrometer, In preparation.

700 Qingguo, H., Liansheng, W., and Shuokui, H.: The genotoxicity of substituted nitrobenzenes and the quantitative structure-activity relationship studies, *Chemosphere*, 30, 915-923, 10.1016/0045-6535(94)00450-9, 1995.

Ravindra, K., Mor, S., and Kaushik, C. P.: Short-term variation in air quality associated with firework events: A case study, *Journal of Environmental Monitoring*, 5, 260-264, 10.1039/b211943a, 2003.

705 Reyes-Villegas, E., Green, D. C., Priestman, M., Canonaco, F., Coe, H., Prévôt, A. S. H., and Allan, J. D.: Organic aerosol source apportionment in london 2013 with me-2: Exploring the solution space with annual and seasonal analysis, *Atmos. Chem. Phys.*, 16, 15545-15559, 10.5194/acp-16-15545-2016, 2016.

Saleh, R., Robinson, E. S., Tkacik, D. S., Ahern, A. T., Liu, S., Aiken, A. C., Sullivan, R. C., Presto, A. A., Dubey, M. K., Yokelson, R. J., Donahue, N. M., and Robinson, A. L.: Brownness of organics in aerosols from biomass burning linked to their black carbon content, *Nat Geosci*, 7, 647-650, 10.1038/NGEO2220, 2014.

710 Sandradewi, J., Prévôt, A. S. H., Szidat, S., Perron, N., Alfarra, M. R., Lanz, V. A., Weingartner, E., and Baltensperger, U. R. S.: Using aerosol light absorption measurements for the quantitative determination of wood burning and traffic emission contribution to particulate matter, *Environmental Science and Technology*, 42, 3316-3323, 10.1021/es702253m, 2008.

715 Sato, K., Takami, A., Iozaki, T., Hikida, T., Shimono, A., and Imamura, T.: Mass spectrometric study of secondary organic aerosol formed from the photo-oxidation of aromatic hydrocarbons, *Atmos Environ*, 44, 1080-1087, 10.1016/j.atmosenv.2009.12.013, 2010.

- 720 Slowik, J. G., Vlasenko, A., McGuire, M., Evans, G. J., and Abbatt, J. P.: Simultaneous factor analysis of organic particle and gas mass spectra: Ams and ptr-ms measurements at an urban site, *Atmos Chem Phys*, 10, 1969-1988, 2010.
- Sun, Y. L., Zhang, Q., Schwab, J. J., Yang, T., Ng, N. L., and Demerjian, K. L.: Factor analysis of combined organic and inorganic aerosol mass spectra from high resolution aerosol mass spectrometer measurements, *Atmos Chem Phys*, 12, 8537-8551, DOI 10.5194/acp-12-8537-2012, 2012.
- 725 Teich, M., van Pinxteren, D., Wang, M., Kecorius, S., Wang, Z., Müller, T., Močnik, G., and Herrmann, H.: Contributions of nitrated aromatic compounds to the light absorption of water-soluble and particulate brown carbon in different atmospheric environments in Germany and China, *Atmos. Chem. Phys.*, 17, 1653-1672, 10.5194/acp-17-1653-2017, 2017.
- 730 Tian, Y. Z., Wang, J., Peng, X., Shi, G. L., and Feng, Y. C.: Estimation of the direct and indirect impacts of fireworks on the physicochemical characteristics of atmospheric pm10 and pm2.5, *Atmos Chem Phys*, 14, 9469-9479, 10.5194/acp-14-9469-2014, 2014.
- 735 Tiitta, P., Leskinen, A., Hao, L., Yli-Pirilä, P., Kortelainen, M., Grigonyte, J., Tissari, J., Lamberg, H., Hartikainen, A., Kuuspallo, K., Kortelainen, A. M., Virtanen, A., Lehtinen, K. E. J., Komppula, M., Pieber, S., Prévôt, A. S. H., Onasch, T. B., Worsnop, D. R., Czech, H., Zimmermann, R., Jokiniemi, J., and Sippula, O.: Transformation of logwood combustion emissions in a smog chamber: Formation of secondary organic aerosol and changes in the primary organic aerosol upon daytime and nighttime aging, *Atmos. Chem. Phys.*, 16, 13251-13269, 10.5194/acp-16-13251-2016, 2016.
- 740 Vassura, I., Venturini, E., Marchetti, S., Piazzalunga, A., Bernardi, E., Fermo, P., and Passarini, F.: Markers and influence of open biomass burning on atmospheric particulate size and composition during a major bonfire event, *Atmos Environ*, 82, 218-225, 10.1016/j.atmosenv.2013.10.037, 2014.
- Vecchi, R., Bernardoni, V., Cricchio, D., D'Alessandro, A., Fermo, P., Lucarelli, F., Nava, S., Piazzalunga, A., and Valli, G.: The impact of fireworks on airborne particles, *Atmos Environ*, 42, 1121-1132, <http://dx.doi.org/10.1016/j.atmosenv.2007.10.047>, 2008.
- 745 Veres, P., Roberts, J. M., Burling, I. R., Warneke, C., de Gouw, J., and Yokelson, R. J.: Measurements of gas-phase inorganic and organic acids from biomass fires by negative-ion proton-transfer chemical-ionization mass spectrometry, *Journal of Geophysical Research: Atmospheres*, 115, n/a-n/a, 10.1029/2010jd014033, 2010.
- 750 Visser, S., Slowik, J. G., Furger, M., Zotter, P., Bukowiecki, N., Canonaco, F., Flechsig, U., Appel, K., Green, D. C., Tremper, A. H., Young, D. E., Williams, P. I., Allan, J. D., Coe, H., Williams, L. R., Mohr, C., Xu, L., Ng, N. L., Nemitz, E., Barlow, J. F., Halios, C. H., Fleming, Z. L., Baltensperger, U., and Prévôt, A. S. H.: Advanced source apportionment of size-resolved trace elements at multiple sites in London during winter, *Atmos. Chem. Phys.*, 15, 11291-11309, 10.5194/acp-15-11291-2015, 2015.
- Wang, L. W., Wen, L., Xu, C. H., Chen, J. M., Wang, X. F., Yang, L. X., Wang, W. X., Yang, X., Sui, X., Yao, L., and Zhang, Q. Z.: Hono and its potential source particulate nitrite at an urban site in north China during the cold season, *Science of The Total Environment*, 538, 93-101, 10.1016/j.scitotenv.2015.08.032, 2015.
- 755 Wang, Y., Zhuang, G., Xu, C., and An, Z.: The air pollution caused by the burning of fireworks during the lantern festival in Beijing, *Atmos Environ*, 41, 417-431, <http://dx.doi.org/10.1016/j.atmosenv.2006.07.043>, 2007.
- 760 Washenfelder, R. A., Attwood, A. R., Brock, C. A., Guo, H., Xu, L., Weber, R. J., Ng, N. L., Allen, H. M., Ayres, B. R., Baumann, K., Cohen, R. C., Draper, D. C., Duffey, K. C., Edgerton, E., Fry, J. L., Hu, W. W., Jimenez, J. L., Palm, B. B., Romer, P., Stone, E. A., Wooldridge, P. J., and Brown, S. S.: Biomass burning dominates brown carbon absorption in the rural southeastern United States, *Geophys Res Lett*, 42, 653-664, 10.1002/2014gl062444, 2015.
- Weingartner, E., Saathoff, H., Schnaiter, M., Streit, N., Bitnar, B., and Baltensperger, U.: Absorption of light by soot particles: Determination of the absorption coefficient by means of aethalometers, *J Aerosol Sci*, 34, 1445-1463, 10.1016/S0021-8502(03)00359-8, 2003.
- 765 Xu, L., Suresh, S., Guo, H., Weber, R. J., and Ng, N. L.: Aerosol characterization over the southeastern United States using high-resolution aerosol mass spectrometry: Spatial and seasonal variation of aerosol composition and sources with a focus on organic nitrates, *Atmos. Chem. Phys.*, 15, 7307-7336, 10.5194/acp-15-7307-2015, 2015.
- 770 Young, D. E., Allan, J. D., Williams, P. I., Green, D. C., Harrison, R. M., Yin, J., Flynn, M. J., Gallagher, M. W., and Coe, H.: Investigating a two-component model of solid fuel organic aerosol in London: Processes, pm1 contributions, and seasonality, *Atmos Chem Phys*, 15, 2429-2443, 10.5194/acp-15-2429-2015, 2015.
- Yuan, B., Liggio, J., Wentzell, J., Li, S. M., Stark, H., Roberts, J. M., Gilman, J., Lerner, B., Warneke, C., Li, R., Leithead, A., Osthoff, H. D., Wild, R., Brown, S. S., and de Gouw, J. A.: Secondary formation of nitrated phenols:

- 775 Insights from observations during the uintah basin winter ozone study (ubwos) 2014, *Atmos. Chem. Phys.*, 16, 2139-2153, 10.5194/acp-16-2139-2016, 2016.
- Zhang, J. K., Cheng, M. T., Ji, D. S., Liu, Z. R., Hu, B., Sun, Y., and Wang, Y. S.: Characterization of submicron particles during biomass burning and coal combustion periods in beijing, china, *Science of The Total Environment*, 562, 812-821, 10.1016/j.scitotenv.2016.04.015, 2016.
- 780 Zhang, M., Wang, X., Chen, J., Cheng, T., Wang, T., Yang, X., Gong, Y., Geng, F., and Chen, C.: Physical characterization of aerosol particles during the chinese new year's firework events, *Atmos Environ*, 44, 5191-5198, <http://dx.doi.org/10.1016/j.atmosenv.2010.08.048>, 2010.
- Zhu, Q., He, L. Y., Huang, X. F., Cao, L. M., Gong, Z. H., Wang, C., Zhuang, X., and Hu, M.: Atmospheric aerosol compositions and sources at two national background sites in northern and southern china, *Atmos. Chem. Phys.*, 16, 10283-10297, 10.5194/acp-16-10283-2016, 2016.
- 785 Zotter, P., Herich, H., Gysel, M., El-Haddad, I., Zhang, Y., Močnik, G., Hüglin, C., Baltensperger, U., Szidat, S., and Prévôt, A. S. H.: Evaluation of the absorption ångström exponents for traffic and wood burning in the aethalometer-based source apportionment using radiocarbon measurements of ambient aerosol, *Atmos. Chem. Phys.*, 17, 4229-4249, 10.5194/acp-17-4229-2017, 2017.

790

#### **Appendix A: Source apportionment solution without modifying the fragmentation table.**

795 Figure A presents results obtained with test2. Figure A.c shows mass spectra of the two chosen solutions; five sources were identified during nbf period: BBOA, HOA, COA, SVOOA and LVOOA. In the case of the bfo period six different sources were identified: BBOA, HOA, COA, factor4 which seems to be a mixed factor with a peak at  $m/z$ 43 (characteristic of SVOOA) and peaks at  $m/z$  55 and  $m/z$  57 (characteristic of HOA), LVOOA and BBOA\_1. BBOA\_1 source appears to be mixed between LVOOA (peaks at  $m/z$ 28 and  $m/z$ 44) and BBOA (peak at  $m/z$ 60). We can see here, that while test2 resulted to be the best way to deconvolve OA sources compared to tests 1,3 and 4, it still shows mixing with SVOOA, LVOOA, and BBOA\_1. Situation that improved when doing OA source apportionment after modifying the fragmentation table in test2\_ON.

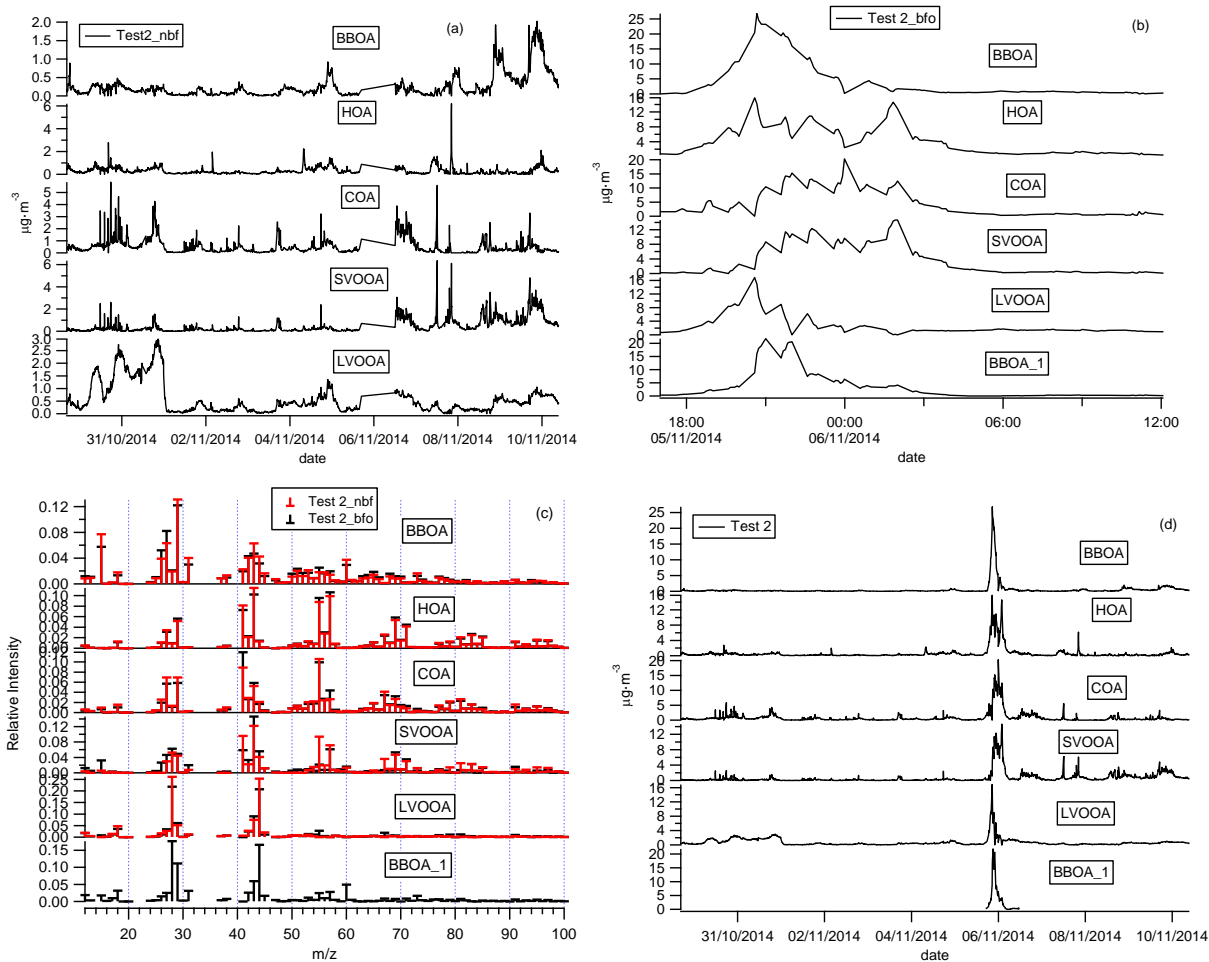


Figure A: OA sources mass spectra and time series for test 2.

#### Appendix B: Symbols and description of main parameters used.

Symbol	Name
<b>Events</b>	
bfo	bonfire-only event (November 05-17:00 hrs – 06 - 12:00 hrs)
nbf	not bonfire (before and after bonfire night)
HSC	High secondary concentrations (October 30th to November 1st)
LC	Low concentrations (November 1st - 3rd )
WL	Winter-like (November 8th -10th)
<b>Aethalometer correction and model</b>	
$\alpha$	Ångström absorption exponent
$\alpha_{tr}$	Ångström absorption exponent for traffic
$\alpha_{wb}$	Ångström absorption exponent for wood burning
ATN	Attenuation
BC	black carbon [ $\mu\text{g}\cdot\text{m}^{-3}$ ]
$b_{abs}$	absorption coefficient [ $\text{m}^{-1}$ ]
$b_{abs\_470}$	absorption coefficient at 470 nm [ $\text{m}^{-1}$ ]
$b_{abs\_950}$	absorption coefficient at 950 nm [ $\text{m}^{-1}$ ]
$\sigma_{ATN}$	attenuation cross section [ $\text{m}^2\cdot\text{g}^{-1}$ ]
$\lambda$	wavelength [nm]
$b_{ATN}$	Uncorrected absorption coefficient [ $\text{Mm}^{-1}$ ]

$b_{abs}$	Corrected absorption coefficient [ $Mm^{-1}$ ]
C	Multiple scattering correction constant
R	Filter loading correction
$f$	shadowing factor
<b>Organic aerosol factors (OA)</b>	
BBOA	Biomass burning organic OA obtained without modifying the fragmentation table
BBOA_1	Second biomass burning organic OA obtained without modifying the fragmentation table
BBOA_2	biomass burning organic OA obtained after modifying the fragmentation table
HOA	Hydrocarbon-like OA
COA	Cooking OA
SVOOA	Semivolatile OA
LVOOA	Low volatility OA
PON	Particulate Organic Oxides of Nitrogen, calculated with 46:30 ratios.
pPON	Primary Particulate Organic Oxides of Nitrogen, estimated using the slope between PON and BBOA
sPON	Secondary Particulate Organic Oxides of Nitrogen, sPON = PON - pPON
pPON_ME2	Primary Particulate Organic Oxides of Nitrogen, calculated from ME-2 analysis
sPON_ME2	Secondary Particulate Organic Oxides of Nitrogen, calculated from ME-2 analysis

805

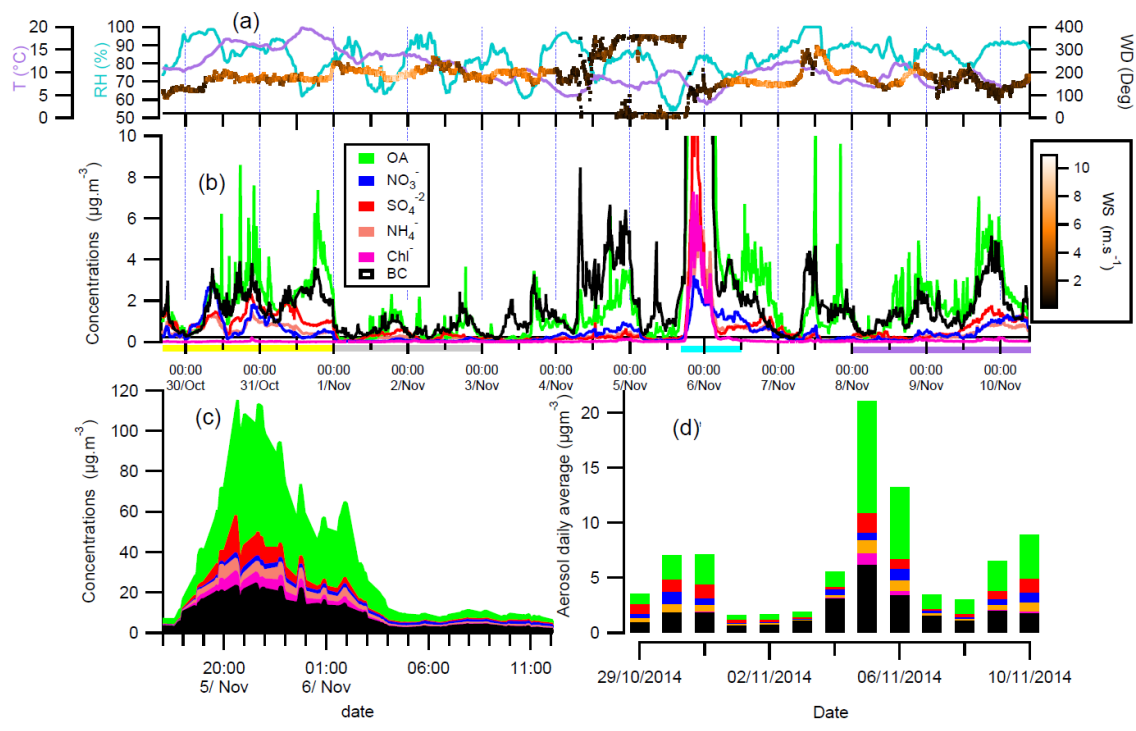
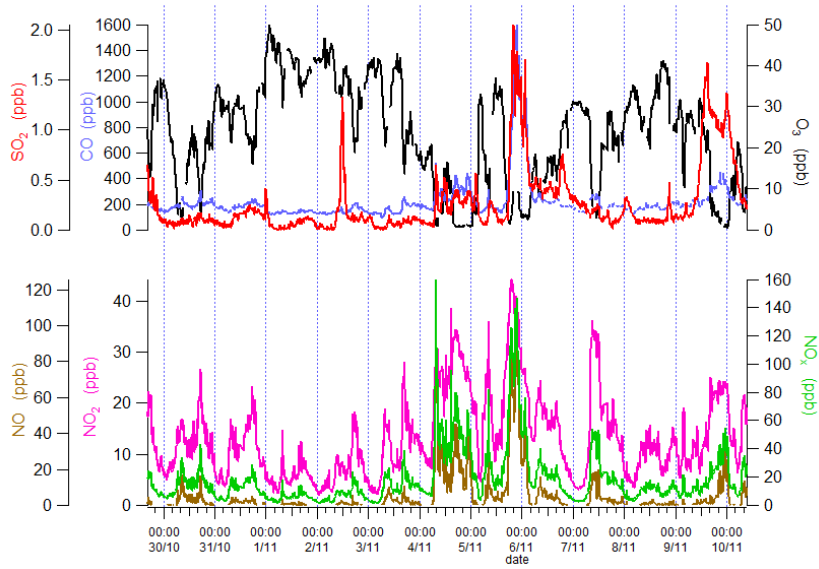


**Figure 1: Meteorology (a), aerosol concentrations during all measurement period (b). Chemical component mass concentrations during Bonfire Night plotted cumulatively (c). Daily aerosol concentrations (d).**



810

Figure 2: Time series of gases measured at Whitworth observatory.

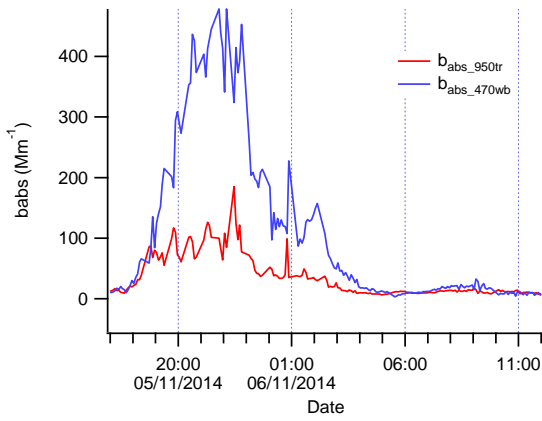


Figure 3: Absorption coefficients for Wood burning (wb) and traffic (tr).

815

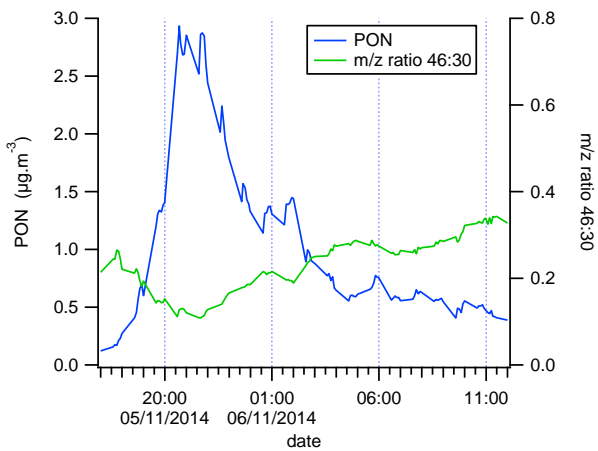
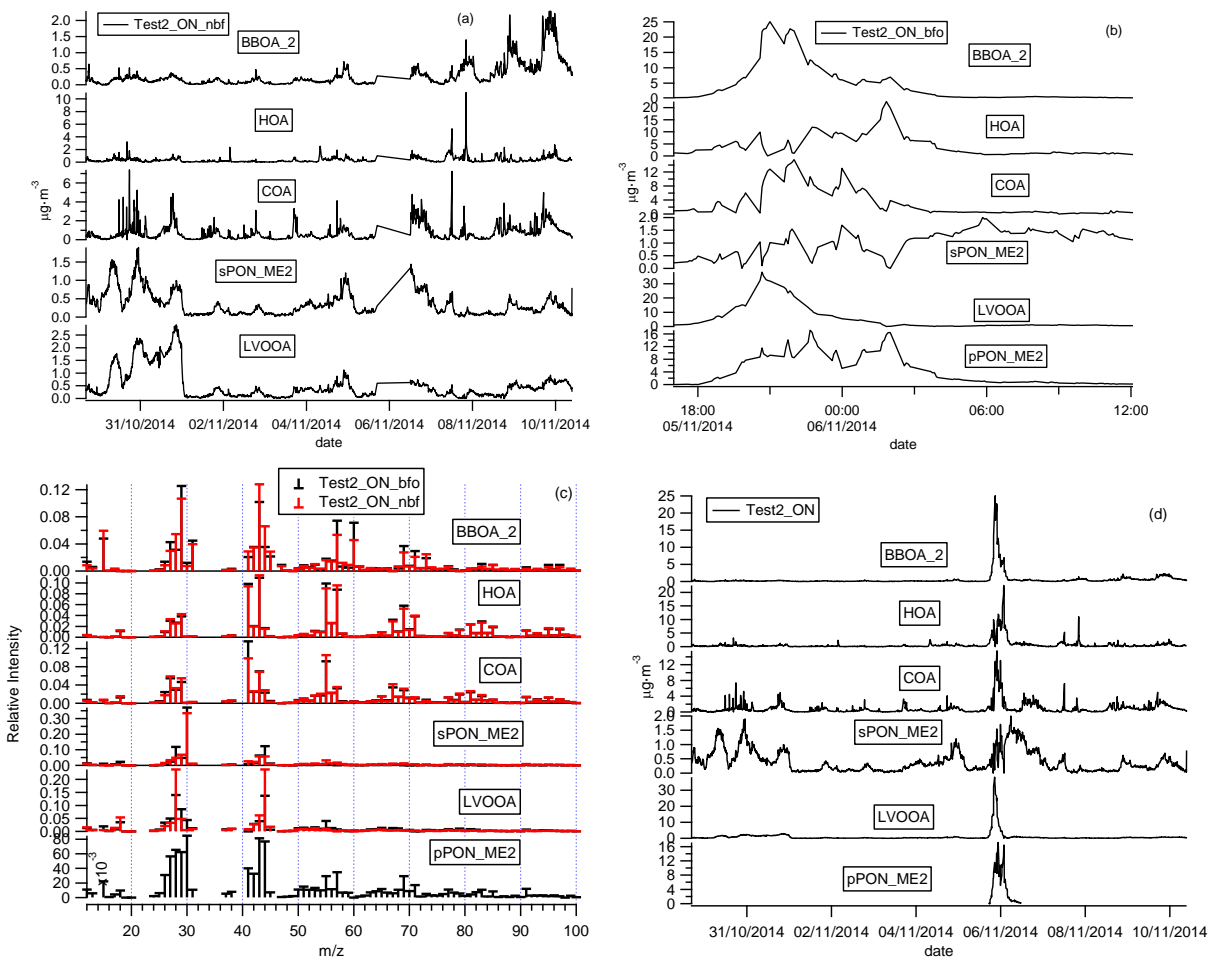
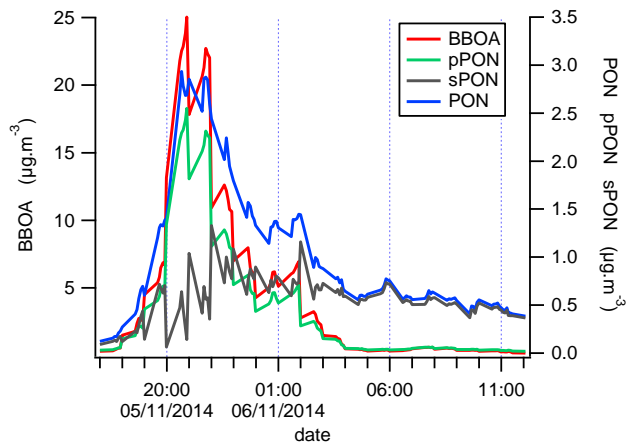


Figure 4: PON concentrations during Bonfire Night.



**Figure 5:** OA sources mass spectra and time series for test 2\_ON for bonfire only (bfo) and not bonfire events (nbf). Figure 6.d shows time series of both events.



**Figure 6:** Secondary (sPON) and primary (pPON) organic nitrate time series estimated from PON and BBOA.

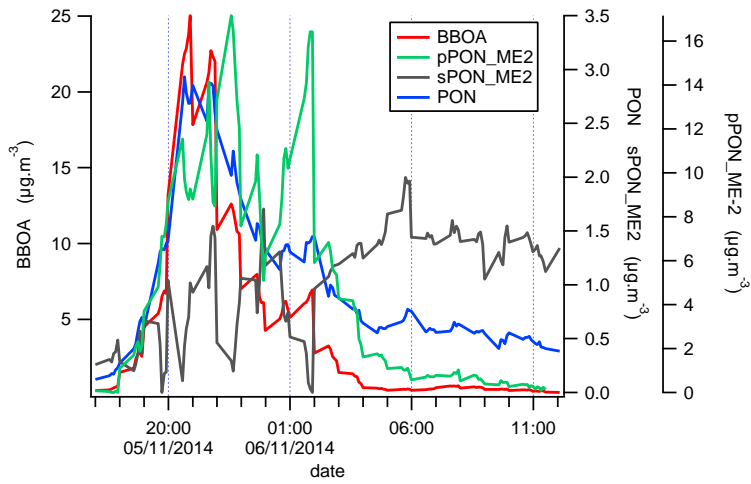


Figure 7: Secondary and primary organic nitrate time series obtained from ME-2 analysis.

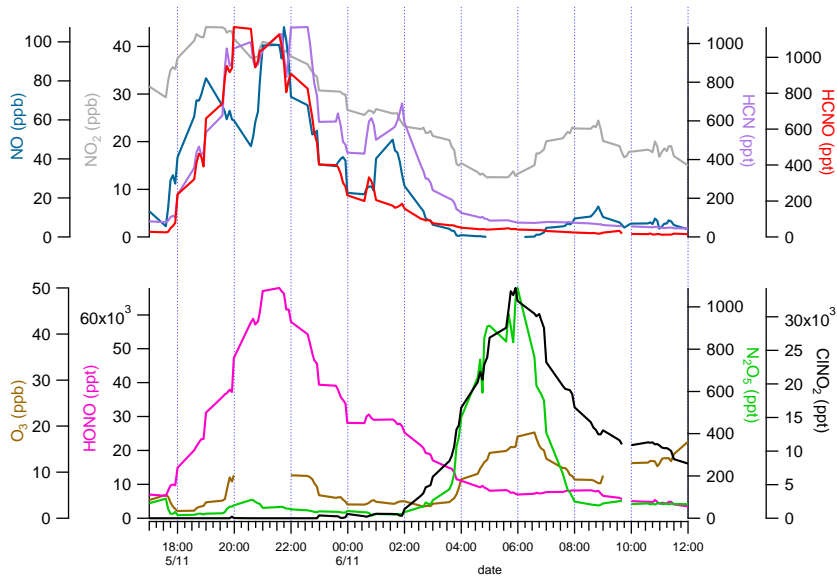


Figure 8: Time series of gases pollutants during Bonfire Night.

Table 1: Multilinear (MLR) and linear regression analysis between  $b_{abs\_470wb}$  and organic aerosols.

			All	HSC	LC	bfo	WL	
MLR 1	A	bkgrd	0.000	4.555	1.004	0.000	1.293	
	B	babs:BBOA	14.340	3.547	18.284	11.926	10.318	
	C	babs:PON	54.495	9.212	12.046	73.115	21.724	
		B/C	0.263	0.385	1.518	0.163	0.475	
		$r^2_{MLR1}$	0.912	0.064	0.364	0.898	0.760	
Linear 1	$r^2$	babs:BBOA	0.861	0.043	0.358	0.839	0.739	
		babs:PON	0.819	0.060	0.275	0.897	0.311	
MLR 2	A	bkgrd	0.000	2.527	0.753	0.000	0.079	
	B	babs:BBOA_2	15.653	27.288	26.481	14.319	10.018	
	C	babs:PON	42.840	0.000	1.200	54.353	18.982	
		B/C	0.365	***	22.060	0.263	0.528	
		$r^2_{MLR2}$	0.922	0.392	0.480	0.902	0.804	
Linear 2	$r^2$	babs:BBOA_2	0.894	0.392	0.480	0.880	0.788	
		babs:PON	0.819	0.060	0.275	0.897	0.311	
MLR 3	A	bkgrd	0.000	2.527	1.649	0.763	6.093	0
	B	babs:BBOA_2	21.545	27.288	22.764	26.668	16.657	8.577
	C	babs:sPON_ME2	3.926	0.000	0.000	0.191	0.000	9.017
	D	D			1.138		7.357	
		B/C	5.488	***	***	***	***	0.951
		B/D			20.005		2.264	
		$r^2_{MLR3}$	0.896	0.392	0.418	0.480	0.910	0.803
Linear 3	$r^2$	babs:BBOA_2	0.894	0.392	0.392	0.480	0.880	0.788
		babs:sPON_ME2	0.024	0.000	0.000	0.273	0.188	0.647
		babs:D			0.225		0.633	

All= complete dataset; HSC= Episode with high secondary concentrations (October 30<sup>th</sup> to November 1<sup>st</sup>), LC = Episode with low concentrations (November 1<sup>st</sup> - 3<sup>rd</sup>); bfo = episode with bonfire only concentrations (05-Nov 17:00 hrs – 06-Nov



12:00 hrs); WL= Episode with winter-like characteristics (November 8<sup>th</sup> -10<sup>th</sup>). PON is the particulate organic nitrate estimate from 46:30 ratios.\*Trilinear regression was performed as in \*bfo analysis there were two PON factors from ME-2 analysis; pPON\_ME2 and sPON\_ME2, with the slope D=babs:pPON and  $r^2_D$  is the  $r^2$  between babs:pPON. In \*HSC analysis; BBOA, sPON and LVOOA were used, with the slope D=babs:LVOOA and  $r^2_D$  is the  $r^2$  between babs:LVOOA.